

Flow-induced breakup of drops and bubbles

Suhas Jain S^{a,1}

^a*Institute of Fluid Dynamics, Helmholtz-Zentrum Dresden-Rossendorf, Germany*

Abstract

Breakup of drop/bubble can be viewed as a result of fundamental force balance when the disruptive force is greater than the restorative force. A disruptive force acting on the drop/bubble tries to deform it, whereas a restorative force refrains it from deforming. Studying breakup and coalescence phenomenon is utmost important since it governs the amount of interfacial area and hence the exchange of heat, mass and momentum across the interface. It also helps in the development of better closure relations for modeling large scale systems.

In this paper, abundant literature consisting of theoretical, experimental and numerical works up to date is reviewed. Broadly, breakup is classified into viscous, inertial and complex turbulent breakup. Physics involved and non-dimensional numbers governing the drop and bubble breakup in various flow configurations are discussed. Characteristic parameters of the breakup such as critical diameter (d_{max}), maximum deformation, breakup time (t_b), wavelength of disturbance (λ), impurities in the flow, initial shape of the drop/bubble, history of the flow and critical values of non-dimensional numbers are examined and the important parameters are listed for ready-to-use in modeling approaches. Finally, scope for future work in number of areas is identified.

Keywords: drop, bubble, viscous & inertial breakup, breakup time, critical diameter, maximum deformation

Email address: sjsuresh@stanford.edu (Suhas Jain S)

¹Presently a graduate student at Center for Turbulence Research, Stanford University, USA

1. Introduction

Flow of a continuous liquid phase containing bubbles or immiscible drops occurs frequently in a large variety of natural phenomena and technical processes. Examples comprise emulsification, extraction, absorption, distillation and boiling which are relevant to food processing, chemical engineering and energy production among others. An understanding of such flows therefore is of high interest since it can lead to predictive models for CFD-simulation that would be useful for scale-up and optimization of the mentioned processes. Progress in this direction is difficult because a wide range of scales is involved with the size of the domain occupied by the two-phase mixture at the large end and the size of the individual drops or bubbles at the small end. Moreover a spectrum of drop or bubble sizes is typically present.

In dispersed multiphase flows, knowledge of the distribution of drop or bubble sizes is a central issue because this distribution determines the interfacial area which in turn determines the interfacial mass, momentum, and energy exchange. Concerning multiphase CFD-simulation these exchange processes have to be modeled within the Eulerian two-fluid framework of interpenetrating continua that is required to facilitate computation on large domains for industrial applications. The evolution of the drop or bubble size distribution in turn is governed by the dynamics of coalescence and breakup processes. Many attempts have been made to include closure models for these processes in the Euler-Euler description of dispersed two-phase flows (Liao and Lucas 2009, 2010, Solsvik et al. 2013). However, no agreement on a suitable one has been reached and the predictive capability is far from satisfactory. In part this state of affairs is due to the fact that both processes compete and only the difference of their rates is observable as a change in the size distribution.

In the present work we take a step back and focus on the available mechanistic understanding of these processes that forms the basis of any modeling work. Of the two, understanding of coalescence appears more advanced to date than understanding of breakup. In addition, coalescence can be suppressed by suitable additives if desired, while no such possibility is known for breakup. Therefore, a viable strategy for Euler-Euler closure modeling is to first consider breakup individually and validate its description for cases where coalescence is suppressed. In a second step the description of coalescence can then be added and validated for cases where both processes occur by keeping the previously developed breakup models fixed. Accordingly, the present work will be limited to the first step and consider only breakup.

Research on deformation and breakup of drops or bubbles has progressed significantly starting from the works of Taylor (1932), but a complete understanding is still not available. Even today new mechanisms causing breakup are being observed both numerically and experimentally for which adequate models are yet to be developed and validated.

A major distinction between the acting mechanisms may be made based on the Reynolds number of the flow. At low Reynolds number, breakup is due to the viscous shear stresses in the external fluid and the breakup depends on the Capillary number, initial shape of the particle undergoing breakup, viscosity ratio and in some cases on the concentration of the impurities in the system. At higher Reynolds number, breakup is due to the inertial forces

acting on the particle and the breakup depends on the Weber number, Ohnesorge number, viscosity ratio and on the shape of the particle undergoing breakup. In the case of turbulent flows, the occurrence of breakup also depends on the complete history of the flow.

Breakup in simple flows is rather well understood. The focus of most of the research in this area has been on the prediction of the critical conditions beyond which no steady drop or bubble shape exists. Breakup criteria are known from the experimental results/theoretical/ numerical models and these serve as the starting point for the further research. Though this method was considered as reasonably successful by various authors, it has failed in describing accurately the critical conditions for breakup.

The current state of understanding of breakup in complex flows in contrast is still meager. For example, the critical Weber number in Kolmogorov-Hinze theory (obtained by balancing the external force with the surface tension force) alone fails to explain the Resonance breakup. Hence further study is required to determine the variables affecting the breakup process in various conditions. The breakup dynamics of the particles in turbulent flow with buoyancy is found to be different from that without buoyancy as observed by Ravelet, Colin and Risso (2011). More detailed studies are yet to be done.

The objective of the present work is to provide a comprehensive review of the literature on the breakup of drops and bubbles. It aims at systematically categorizing and describing all the mechanisms involved in a complete understanding of breakup phenomena, which is crucial for the understanding of dispersed multiphase flows and the development of closure relations for two-fluid models. In this way also a list of the relevant parameters influencing the breakup is obtained. In particular, new findings on breakup in turbulent flows are emphasized and needs for future work in this area are identified. Inevitably there is some overlap with the previous reviews of Stone (1994), Gelfand (1996), Risso (2000), and Ashgriz (2011) to make this article self-contained. The presentation is limited to simple Newtonian fluids. Topics such as breakup up in the presence of surfactants or in electric and magnetic fields or non-Newtonian effects are not considered here. A review on surfactant effects has been given by Stone & Leal (1990), the presence of electric fields has been considered e.g. by Ha & Yang (2000), and non-Newtonian effects are discussed in the book by Chabra (1990, Chap. 6.8).

Drops and bubbles share many features. In fact, they are distinguished only by values of the density- and viscosity-ratio relative to the continuous liquid being small (for bubbles) or not (for drops) which really means a gradual variation. For air bubbles in water for example the ratio of the dynamic viscosities of air to water is about 0.02. As will be seen this is not negligible in some circumstances. The term “particle” will therefore be used further on to refer to either a drop or bubble. As much as possible results are expressed in terms of dimensionless numbers.

Frequently appearing ones are the Reynolds number, Weber number, Capillary number, Ohnesorge number, Bond number (Eötvös number), Archimedes number, Galilei number, viscosity-ratio, where the viscosity ratio is defined as the ratio of the dynamic viscosity of the internal fluid to that of the external fluid,

$$\lambda = \frac{\mu_d}{\mu_c} \quad (1)$$

Reynolds number is defined as the ratio of momentum force to viscous force,

$$Re = \frac{\rho_c U d}{\mu_c} \quad (2)$$

Weber number is defined as the ratio of inertial force to surface tension force,

$$We = \frac{\rho_c U^2 d}{\sigma} \quad (3)$$

Ohnesorge number is defined as the ratio of viscous force to the geometric mean of inertial and surface tension force,

$$Oh = \frac{\mu_d}{\sqrt{\rho_d \sigma d}} = We^{\frac{1}{2}} Re^{-1} \quad (4)$$

Capillary number is defined as the ratio of the viscous force to that of surface tension force acting across an interface,

$$Ca = \frac{\mu_c U}{\sigma} = We Re^{-1} \quad (5)$$

Bond number (Eötvös number) is defined as the ratio of the body force to that of the surface tension force acting across an interface,

$$Eo = Bo = \frac{\Delta \rho g d^2}{\sigma} \quad (6)$$

Archimedes number (Galilei number) is defined as the ratio of the buoyancy force to the viscous force,

$$Ga = Ar = \frac{\rho_c g^{\frac{1}{2}} d^{\frac{3}{2}}}{\mu_c} \left(1 - \frac{\rho_c}{\rho_c}\right) \quad (7)$$

2. Viscous force driven breakup

At low Re values, inertial forces on the particle can be neglected and the particle deformation and breakup are primarily due to the viscous shear stresses. This situation generally applies to the breakup of small particles in highly viscous liquids. Acrivos (1983), Rallison (1984), Stone (1994), and Risso (2000) have extensively reviewed this area.

When inertia is negligible, flow is governed by the Stokes' equations. Dimensional analysis of these governing equations reveals that the flow is governed majorly by the λ and Ca .

Close observation at results of the theoretical and experimental studies has also revealed that the history of the external force and the initial shape of the particle also play a major role. Further, breakup of this kind can be classified as steady and unsteady based on the characteristics of external flow:

2.1. Steady flows

This section deals with the breakup in quasi-steady flows. Plane flows of the form

$$\nabla U = \frac{G}{2} \begin{bmatrix} 1 + \alpha & 1 - \alpha & 0 \\ -1 + \alpha & -1 - \alpha & 0 \\ 0 & 0 & 0 \end{bmatrix} \quad (8)$$

are considered, where G is the strength of the external flow and α is a flow type parameter such that $\alpha = +1$ results in a pure straining flow, $\alpha = 0$ a simple shear flow and $\alpha = -1$ a purely rotational flow. Examples of streamline patterns for $\alpha \geq 0$ are shown in Figure 1. Values of $\alpha < 0$ have not been considered in this review.

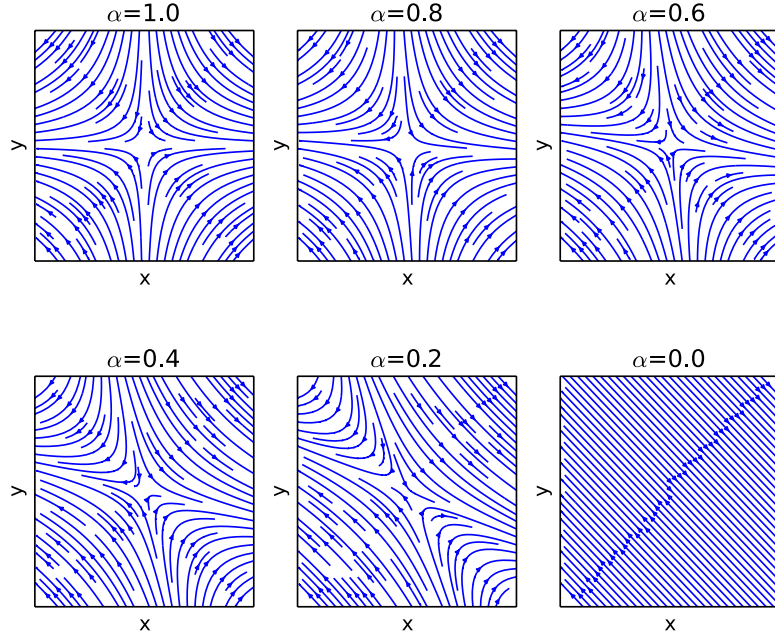


Figure 1: Streamlines of flow field for $\alpha \geq 0$.

If exposed to a flow of the type above an initially spherical particle assumes a prolate ellipsoidal shape as sketched in Figure 2. The measure of deformation $De = (L - B)/(L + B)$ is frequently used for small deformations. At large deformations, it tends to a limiting value of 1 by definition so it ceases to be useful. In this case $\frac{L}{a} = \left(\frac{1+De}{1-De}\right)^{\frac{2}{3}}$ (assuming a prolate ellipsoidal shape) has to be used, which has no restrictions on its applicability.

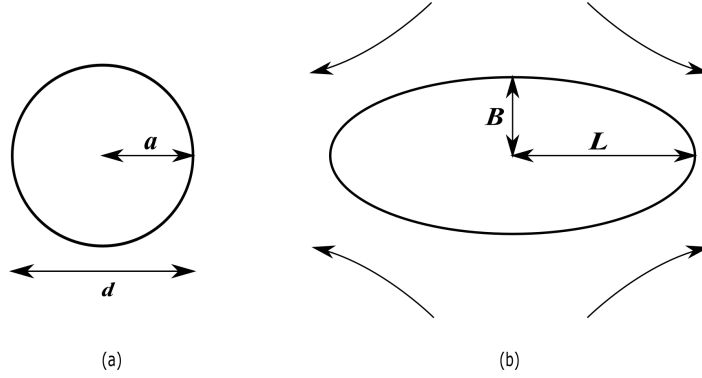


Figure 2: Particle morphology. (a) Initial spherical particle. (b) Particle shape under the influence of external flow field.

Viscosity ratio has a marked effect on the morphology of the particles. Hence based on this, study is further divided into high, medium and low viscosity ratio flows.

2.1.1. High viscosity ratio flows

At high viscosity ratios, $\lambda \sim 1$ or larger, the disruptive viscous forces tend to breakup the particles at relatively low shear rates or at moderate deformations.

Very first studies on this were done by Taylor (1932, 1934). He considered an almost spherical particle in a simple shear flow ($\alpha = 0$) and calculated the flow field around it by balancing the largest value of the pressure difference occurring on the particle surface with the average stresses due to surface tension. He obtained an estimate for the maximum stable initial radius of the particle, given by

$$a = \frac{2\sigma(\mu_d + \mu_c)}{G(1 + \alpha)\mu_c(\frac{19}{4}\mu_d + 4\mu_c)} \quad (9)$$

which can be rewritten in terms of critical capillary number as

$$Ca_{crit} = \frac{2(\lambda + 1)}{(1 + \alpha)(\frac{19}{4}\lambda + 1)} \quad (10)$$

Taylor (1934) also performed experiments using a parallel band apparatus on the deformation of a particle of one fluid in another with controlled interfacial tension, viscosities, and rate of deformation of the outer fluid and showed that the experiments matched well with his theory (Taylor 1932) at low shear rates.

Further, Cox (1969) worked on theoretically determining the shape of the particle in simple shear and pure straining flows by assuming the particle deformation to be small and of order $\epsilon \ll 1$ and expanding the velocity field in terms of this parameter. But their model failed to indicate the possibility of breakup. Torza et al. (1972) conducted experiments on

neutrally buoyant liquid particles suspended in viscous liquids undergoing simple shear flow and validated the model developed by Cox (1969).

Cox (1969)'s theoretical work was further extended by Frankel and Acrivos (1970), Barthes-Biesel (1972) and Barthes-Biesel and Acrivos (1973). They used linear stability theory to predict the onset of breakup of particles freely suspended in a simple shear flow and found that the results were in good agreement with the experimental works of Taylor (1934), Rumscheidt and Mason (1961) and Grace (1971).

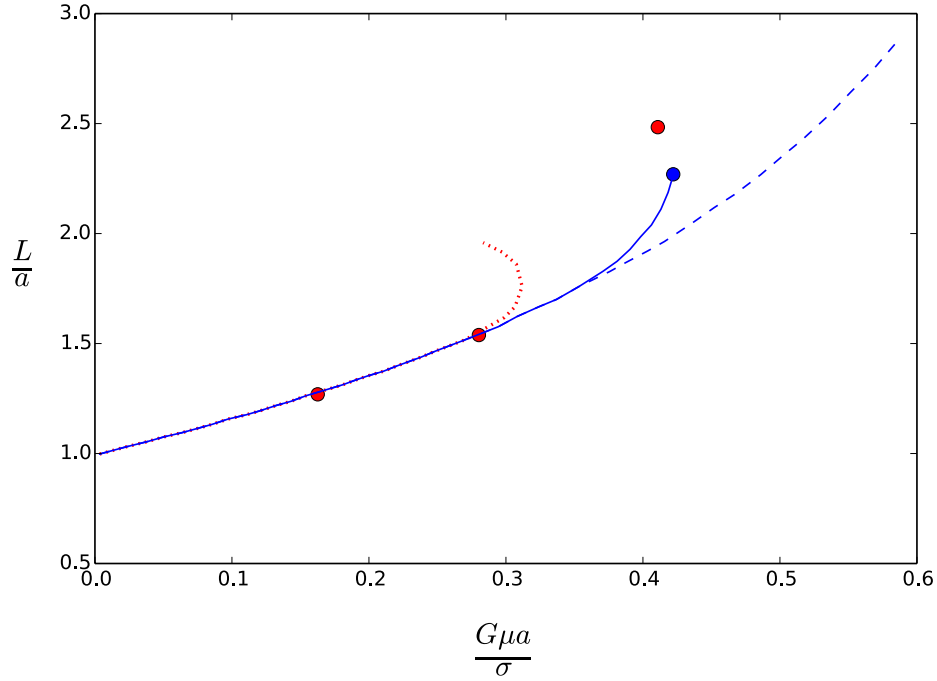


Figure 3: Elongation ratio $\frac{L}{a}$ of a particle in simple shear flow when $\lambda = 1$ [Redrawn from Figure 4 in Acrivos (1983)]. Solid line: numerical results obtained by Rallison (1981). Filled blue circle: the numerically determined point of breakup. Filled red circles: experimental measurements by Rumscheidt and Mason (1961). Dashed line: theory by Taylor (1932). Dotted line: theory by Barthes-Biesel and Acrivos (1973).

Figure 3 summarizes the works on high viscosity ratio flows,

- Taylor's theory is accurate in determining the deformation up to the point of breakup, though it doesn't predict critical shear rate for breakup.
- Theory by Barthes-Biesel and Acrivos (1973) over predicts the deformation but describes the critical shear rate at an acceptable accuracy for $\lambda \geq 0.05$ (provides a good qualitative picture but not in good quantitative agreement).
- Breakup was obtained by a non-existence of a steady solution for the system of equations.

- There is excellent agreement between the calculated deformations and those found experimentally, up to the point of breakup.

2.1.2. Low viscosity ratio flows

On the other hand, for low viscosity ratios, the particles are highly elongated and slender, i.e. $L \gg B$. Taylor (1964) was the first to calculate the particle deformation in the slender body limit. He calculated the effect of presence of a particle on the pure straining flow by a distribution of singularities along the particle axis and calculated the type, strength and position of these singularities together with the position of the particle axis that matched the boundary conditions. Buckmaster (1972, 1973) refined this theory considering inviscid particles in axisymmetric pure straining flow of a highly viscous fluid and further Acrivos and Lo (1978) extended it for low but finite viscosity particles. Hinch and Acrivos (1980) solved for simple shear flows and Khakhar and Ottino (1986) have also contributed to this theory.

Slender body theory only applies to $\lambda \ll 1$ at the main central region of the particle and not near the pointed ends of the particle. The deformation relation is given by

$$10\left(\frac{G\mu a\lambda^{1/6}}{\sigma}\right)^2 = \frac{L\lambda^{\frac{1}{3}}}{a} / \left(1 + \frac{4}{5}\left(\frac{L\lambda^{1/3}}{a}\right)^3\right)^2 \quad (11)$$

and is shown in Figure 4.

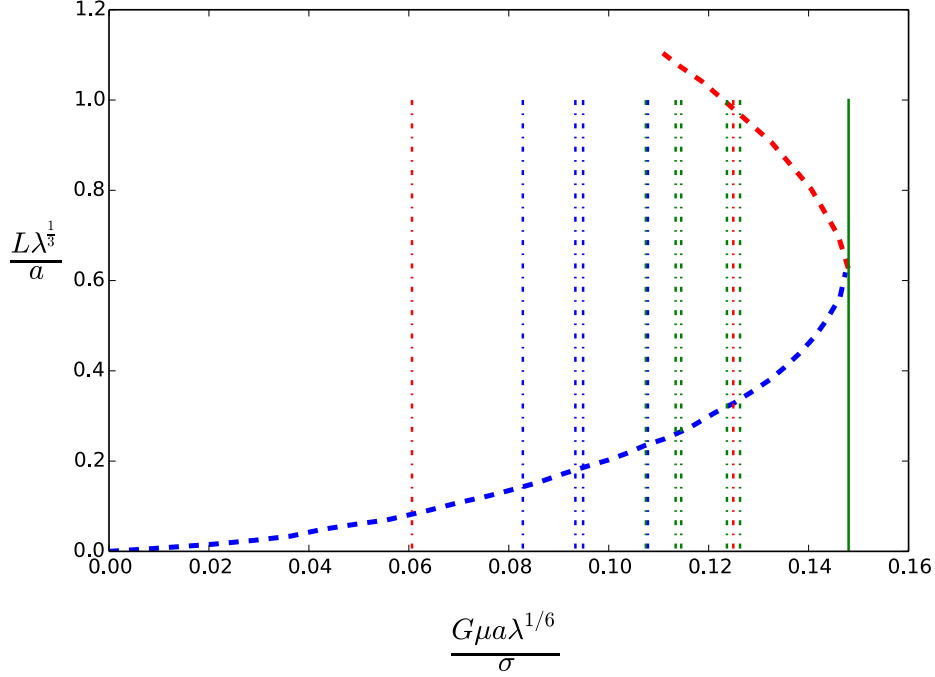


Figure 4: Blue and red dashed line: deformation and breakup of a particle of very low viscosity ($\lambda \ll 1$) in pure straining flow, Solid green line: critical value of G for breakup, Blue dash-dotted line: experimental critical value of G for breakup at $\mu_c = 45.5P$ by Grace (1971), Red dash-dotted line: experimental critical value of G for breakup at $\mu_c = 502.5P$ by Grace (1971), Green dash-dotted line: experimental critical value of G for breakup at $\mu_c = 502.5P$ by Yu (1974) [Redrawn from Figure 6 in Acrivos (1983) and Figure 4 in Hinch and Acrivos (1979)].

A more physical explanation is that an increase in the shear rate G leads to a decrease in the local cross-sectional radius of the particle, since the capillary forces must balance the external shear stress; this, in turn, leads to an increase in L and corresponding decrease in the pressure within the particle at its center, which requires a further decrease in the radius. Clearly, this cannot continue indefinitely and for large enough values of G the particle breaks.

Hinch and Acrivos (1979, 1980) extended this analysis to pure straining flows and to simple shear flows. In the former case, they found that, although the cross-section of the particle becomes significantly distorted from the circular shape, the deformation curve remained essentially similar as in axisymmetric flows and breakup is predicted to occur when $\frac{G\mu a\lambda^{1/6}}{\sigma}$ reaches a value equal to 0.145, rather than 0.148, as in axisymmetric flow and that there is good agreement between this theoretical criterion for breakup and the experimental observations as shown in Figure 4. In the latter case of simple shear flow, the situation was much more complex and only qualitative agreement with the experiment was obtained.

2.1.3. Medium viscosity ratio flows

Bentley and Leal (1986) conducted an experimental investigation of particle deformation and breakup (Figure 5) in a simple flow field conforming to the Eq. 8 with the values of $\alpha = 1.0, 0.8, 0.6, 0.4, 0.2$. Their most important result is the critical capillary number $Ca_{crit} = \frac{G\mu a}{\sigma}$ as a function of viscosity ratio λ and the flow parameter α (Figure 6). This critical value depends on the flow history (1972 Torza, 1971 Grace). Hence, the flow rate was increased very slowly so that the particle undergoes a sequence of quasi-equilibrium states and any other conditions would breakup the particle at lower rate. Breakup was said to occur at that flow rate where no stationary particle shape existed anymore. Figure 7 shows the deformation of the particles for conditions up to breakup. Finally, a reasonable agreement was achieved with small deformation theory ($\lambda > 0.05$) and slender body theory ($\lambda \leq 0.01$).

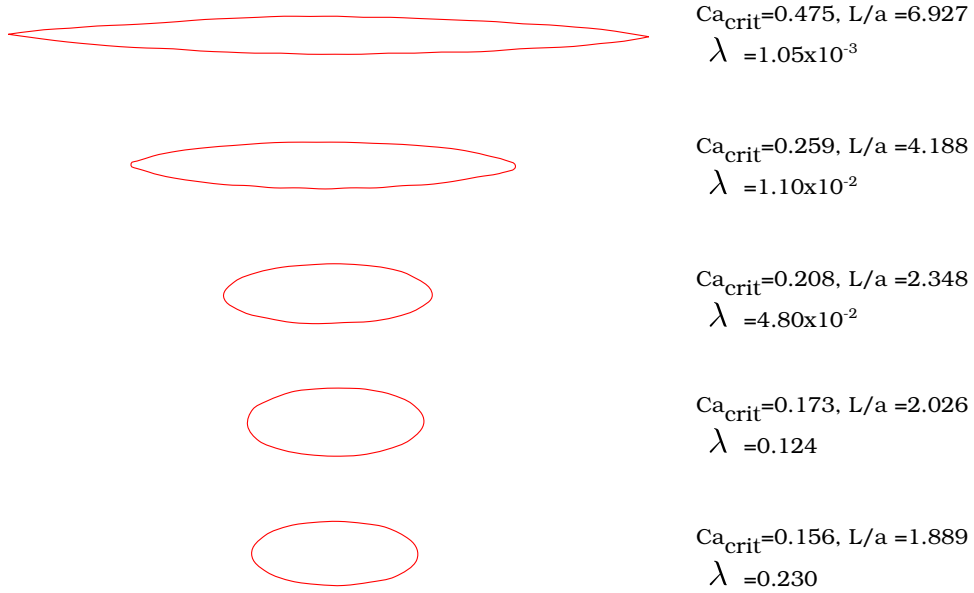


Figure 5: Most extended stable shapes for each viscosity ratio investigated at $\alpha = 1$. [Outlines extracted from experimental photographs of Bentley and Leal (1986)].

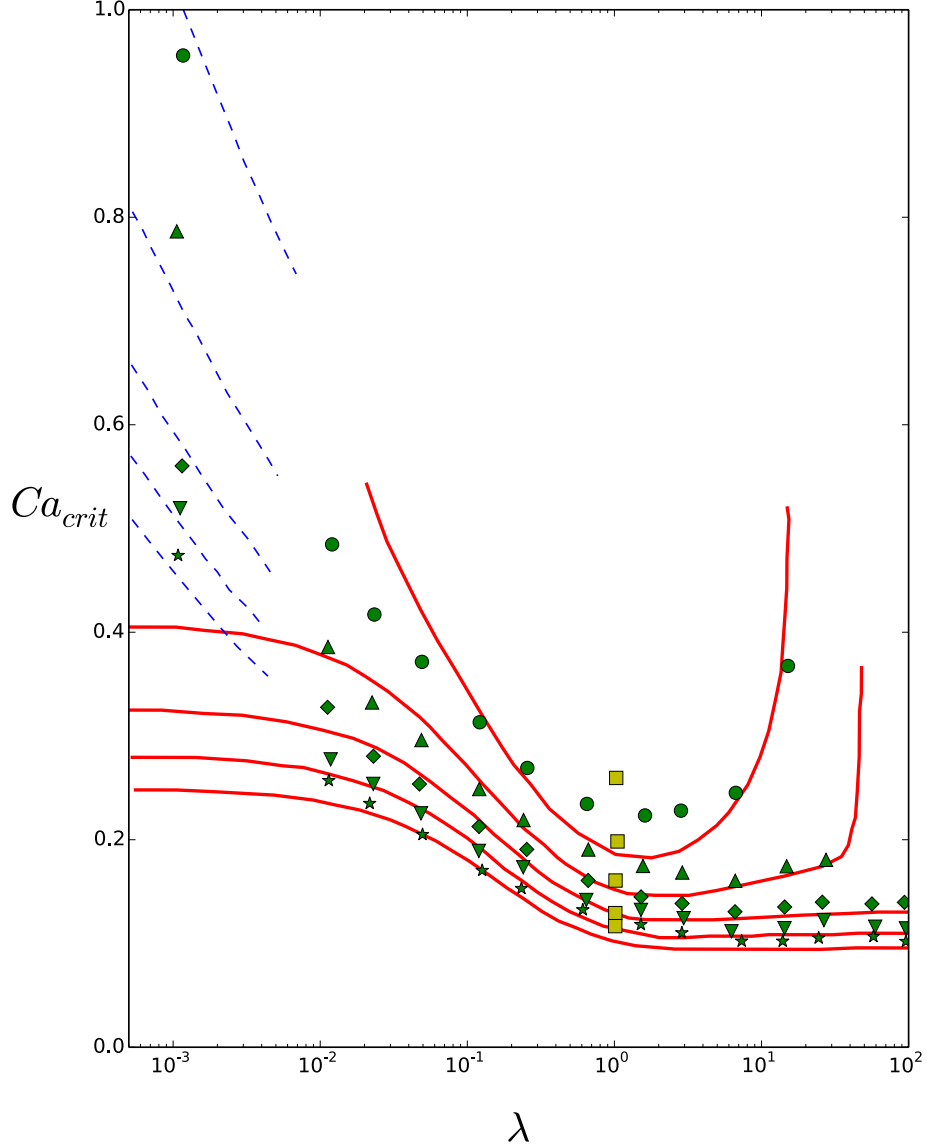


Figure 6: Critical capillary number vs viscosity ratio for different values of α . Values of α (0.2, 0.4, 0.6, 0.8 and 1.0) increases from top to bottom. Solid line: small-deformation theory, Dashed line: large-deformation theory, Green circles: $\alpha = 0.2$, Green upward triangles: $\alpha = 0.4$, Green diamonds: $\alpha = 0.6$, Green downward triangles: $\alpha = 0.8$, Green stars: $\alpha = 1.0$, Yellow squares: results obtained by Rallison (1981) [Redrawn from the Figure 28 in Bentley and Leal (1986)].

Figure 6 shows the Ca_{crit} number for all five flow types investigated. For high viscosity ratios ($\lambda > 1$), there is a strong qualitative dependence on the flow type which is quite well predicted by small deformation theory (solid lines) and can be represented by an approximate relation $Ca_{crit} = 0.127\alpha^{-\frac{3}{4}}\lambda^{0.13\alpha}$. For low viscosity ratios ($\lambda < 1$), the behavior is

qualitatively similar for all the flow types but quantitative differences within a factor 2 to 3 are seen and can be expressed by an analytical relation $Ca_{crit} = 0.1457\alpha^{-\frac{1}{2}}\lambda^{-\frac{1}{6}}$. The ad hoc generalization of large-deformation theory (dashed lines) predicts breakup with acceptable accuracy for the medium λ values in the absence of theoretical data.

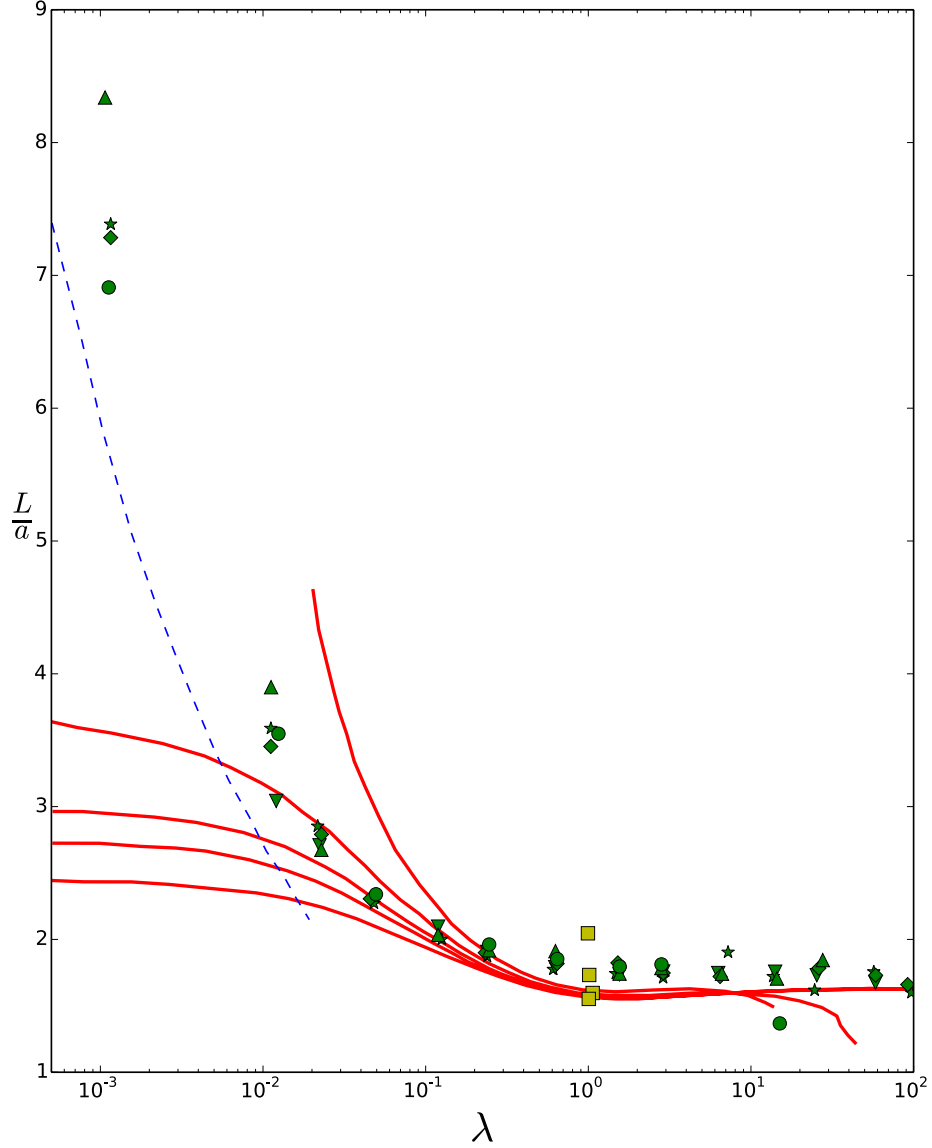


Figure 7: Elongation ratio $\frac{L}{a}$ vs viscosity ratio for different values of α . Values of α (0.2, 0.4, 0.6, 0.8 and 1.0) increases from top to bottom. Solid line: small-deformation theory, Dashed line: large-deformation theory (same for all values of α), Green circles: $\alpha = 0.2$, Green upward triangles: $\alpha = 0.4$, Green diamonds: $\alpha = 0.6$, Green downward triangles: $\alpha = 0.8$, Green stars: $\alpha = 1.0$, Yellow squares: results obtained by Rallison (1981) (values for $\alpha = 0.8$ and $\alpha = 1.0$ coincide) [Redrawn from the Figure 29 in Bentley and Leal (1986)].

Figure 6 and Figure 7 can be summarized as follows:

- For $\lambda < 0.02$, the ends of the particle become pointed. Higher the Ca , more is the

particle elongation. Very large deformations and capillary numbers are required to cause the breakup at this λ values.

- For $\lambda > 0.02$, the ends remained rounded up to breakup. Higher the viscosity ratio, smaller are the maximum stable deformation and Ca_{crit} .
- For $\lambda > 3$, the central portion of the particle become cylindrical. There exists a value of λ beyond which the breakup becomes impossible and the particle deformation does not increase any more with increasing Ca .

The steady, viscous driven breakup of the particles in simple flows is one of the earliest areas to be extensively studied and comparatively well understood. Hence, it has been accounted in brief and a detailed review would be just repetitive.

2.2. Unsteady flow

Most of the present day research in the viscous driven breakup is directed towards understanding the phenomenon in unsteady external flows.

In an assumed stationary case, for sufficiently small values of the Ca , a steady particle-shape exists in a steady two-dimensional flow for all the values of λ . But in the majority of cases there exists a Ca_{crit} , above which a steady particle shape no longer exists and the viscous forces continually elongate the particle. After the particle has reached a given elongation, if the flow magnitude is suddenly decreased to a sub-critical value $Ca_a < Ca_{crit}$, the particle relaxes towards the steady shape corresponding to the final capillary number Ca_a . If the initial elongation was longer than a critical value, breakup occurs in such a time-dependent situation. Figure 8 denotes the summary of the effect of elongation ratio on the break-up of the particle.

Figure 8 also shows a difficulty in particle breakup for high and low viscosity ratios. These are the observations of the experiments made by Stone, Bentley & Leal (1986) for the case of drops. This was further extended to the case of bubbles by Kang and Leal (1987). They did axisymmetric computations of bubbles in pure straining flow and observed the critical elongation ratio as 2.01 at $Re_c = 10$, 1.542 at $Re_c = 100$ and 1.272 at $Re_c = \infty$.

2.2.1. Capillary wave instability

Plateau (1873) identified an instability in cylindrical threads due to surface tension and he proposed that a liquid cylinder under the influence of surface tension was unstable if its length was as long as its circumference. Later, Rayleigh (1879) found that a liquid jet is unstable for axial disturbances (axisymmetric disturbances) with wave numbers less than a cut-off value k_c . Since the forces that are acting on the disturbed interface are the surface tension or the capillary forces, he referred to waves as the capillary waves.

Initial theory by Rayleigh (1879) assumed an inviscid infinite liquid jet neglecting the surrounding gas effects (inviscid surrounding media) and derived a simple characteristic relationship between the wavenumber and growth rate (Figure 9). The maximum growth rate occurs at $ka = 0.697$. For each wavelength of unstable disturbance, one main particle and one or more usually smaller particles are formed. This theory is valid only for small

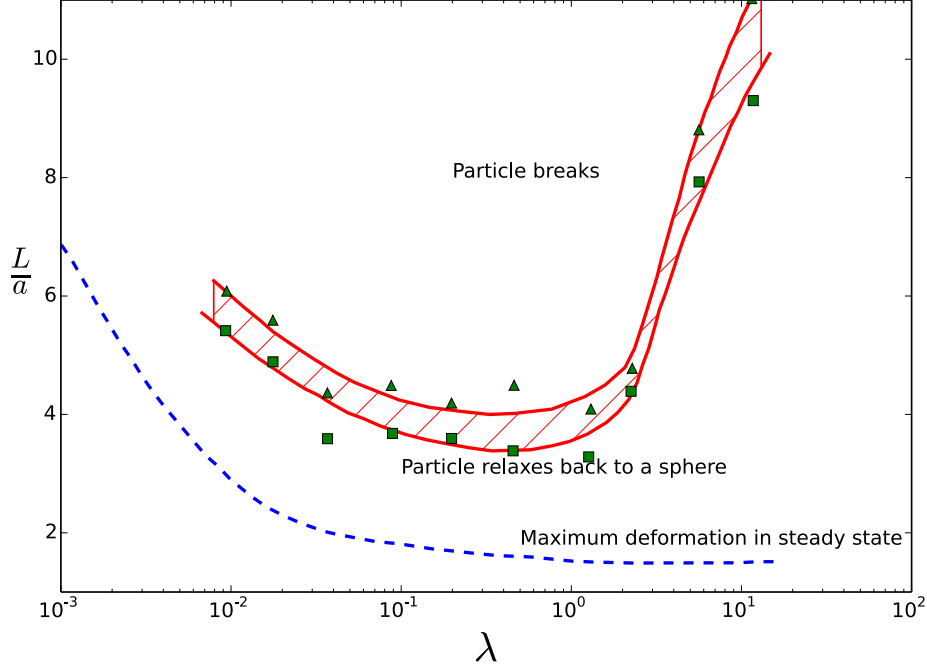


Figure 8: Squares: max stable critical elongation ratio $\frac{L}{a}$ for the particle to relax back, Triangles: minimum $\frac{L}{a}$ for the particle to break, Hatched area: shows the uncertainty in critical elongation ratio, Dashed line: elongation ratio for the most deformed particle in steady state observed experimentally by Bentley and Leal (1986). [Redrawn from the Figure 12 in Stone, Bentley & Leal (1986)].

disturbances acting on the interface and also provides an estimate of the daughter particle size emerging from the breakup.

Weber (1931) and Chandrasekhar (1961) extended the Rayleigh's theory to viscous liquid jets and explained that the viscosity of the jet dampens the instability and shifts the fastest growing perturbations toward longer waves as shown in the Figure 9.

Tomotika (1935) further extended the work of Rayleigh (1879, 1892) to viscous liquid threads surrounded by another viscous fluid based on the experiments in Taylor (1934). They considered both the inside and outside fluids to be at rest and derived a general equation for the relation between the growth rate n and ka given by,

$$\begin{vmatrix} I_1(ka) & I_1(k_{d1}a) & K_1(ka) & K_1(k_{c1}a) \\ kaI_0(ka) & k_{d1}aI_0(k_{d1}a) & -kaK_0(ka) & -k_{c1}aK_0(k_{c1}a) \\ \frac{2\mu_d}{\mu_c}k^2I_1(ka) & \frac{\mu_d}{\mu_c}(k^2 + k_{d1}^2)I_1(k_{d1}a) & 2k^2K_1(ka) & (k^2 + k_{c1}^2)K_1(k_{c1}a) \\ F_1 & F_2 & F_3 & F_4 \end{vmatrix} = 0 \quad (12)$$

where $K_n(x)$ and $I_n(x)$ are n^{th} order modified Bessel functions and,

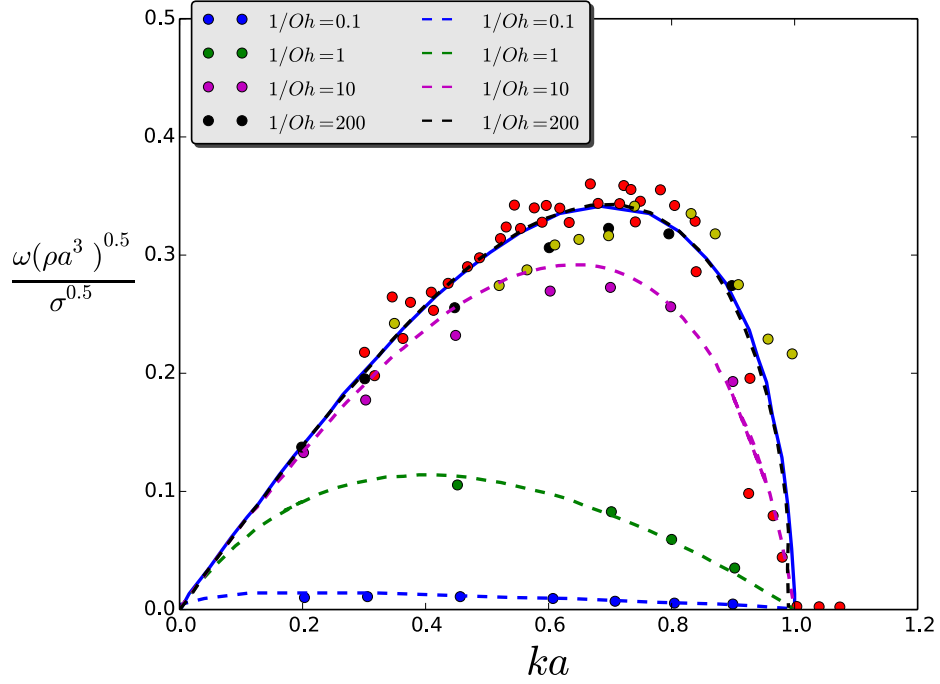


Figure 9: Non-dimensional growth rate vs the wave number. Red dots: Goedde and Yuen (1970), Blue solid-line: Theoretical result of Rayleigh (1879), Yellow dots: Experimental data from Cline and Anthony (1978), Blue, Green, Magenta and Black dots: Numerical results of Ashgriz and Mashayek (1995). Blue, Green, Magenta and Black dashed-lines: Corresponding theoretical results of Chandrashekar (1961).

$$\left. \begin{aligned} k_{c1}^2 &= k^2 + \frac{in}{\nu_c} \\ k_{d1}^2 &= k^2 + \frac{in}{\nu_d} \end{aligned} \right\} \quad (13)$$

$$\left. \begin{aligned} F_1 &= 2i \frac{\mu_d}{\mu_c} k^2 I_1'(ka) - \frac{n\rho_d}{\mu_c} I_0(ka) + \frac{T(k^2 a^2 - 1)}{a^2 n \mu_c} k I_1(ka), \\ F_2 &= \frac{2i\mu_d}{\mu_c} k k_{d1} I_1'(k_{d1}a) + \frac{T(k^2 a^2 - 1)}{a^2 n \mu_c} k I_1(k_{d1}a) \\ F_3 &= 2ik^2 K_1'(ka) + \frac{n\rho_c}{\mu_c} K_0(ka) \\ F_4 &= 2ik k_{d1} K_1'(k_{c1}a) \end{aligned} \right\} \quad (14)$$

If the inertia effects are assumed insensible when compared to viscous effects, the equation can be reduced by applying $\rho_d \rightarrow 0$ and $\rho_c \rightarrow 0$.

Limiting solutions. When viscosity ratio was assumed to be infinity, the equation set reduced to,

$$in = \frac{T(k^2a^2 - 1)}{2a\mu_d \left(k^2a^2 + 1 - \frac{k^2a^2 K_0^2(ka)}{I_1^2(ka)} \right)} \quad (15)$$

which is identical to Rayleigh (1892) solution. Max value of in is achieved when $ka \rightarrow 0$. Therefore maximum instability when the wavelength of varicosity is very large compared to the radius of the column.

When viscosity ratio was assumed to be tending to zero, the equation set reduced to,

$$in = \frac{T(1 - k^2a^2)}{2a\mu_c \left(k^2a^2 + 1 - \frac{k^2a^2 K_0^2(ka)}{K_1^2(ka)} \right)} \quad (16)$$

Similarly, even here, max value of in is when $ka \rightarrow 0$. Therefore, maximum instability when the wavelength of varicosity is very large compared to radius of the column.

For a general case, max value of in was attained for $ka = 0.568$, which corresponds to a wavelength of $5.53 \times 2a$. They validated their theory by comparing this to a value of $ka = 0.5$ which was obtained from experiments in Taylor (1934). For a more general treatment of limiting cases and its applicability, refer Meister and Scheele (1967). They also gave a generalized correlation for wave number ka and the disturbance of growth rate for liquid-liquid system for a wide range of viscosity ratio and density ratio values in Figures 6-9 in Meister and Scheele (1967).

Another observation made by experimental studies of Taylor (1934) was that if the apparatus were kept going, very much smaller particles were formed than if it were stopped as soon as the initial particle had been pulled out into a cylindrical thread, which implied a stabilizing effect of the flow in the surrounding fluid. This concept was theoretically analyzed by Tomotika (1936) along the similar lines of Tomotika (1935), except that both the thread and surrounding fluid was stretched at a uniform rate in an axisymmetric pure straining flow as in the experiments of Taylor (1934) and inertial effects were neglected when compared to viscous effects. They showed that the flow in surrounding fluid limits the growth of any initial disturbance to a finite value and proved this theoretically using the relative growth of disturbance, wherein the value of this relative growth of amplitude of varicosity(disturbance) was 1 : 20.89 for a cylindrical thread which was just formed from an initial particle and 1 : 2.26×10^{10} for a particle drawn into $\frac{1}{8th}$ of initial diameter. This theory was experimentally validated by Rumscheidt and Mason (1962). They found a good agreement for wavelengths and rates of disturbances for the systems with viscosity ratios of 0.03 to 6.7 with the theory. This theory was further extended by Mikami, Cox and Mason (1975) with the help of experiments on the breakup of liquid threads in pure straining flow.

Stone, Bentley and Leal (1986) observed that when the flow was on, there was no evidence of capillary waves in the central cylindrical section of less extended particles. This is because of the fact that the timescale of end pinching mechanism (Section 2.2.2) is much smaller

than the growth of capillary waves and hence the time taken by the initial infinitesimal disturbance to reach the half cylinder is much larger than the end-pinching mechanism. But if the particle is very highly stretched, fragmentation occurs at the end owing to end pinching mechanism whereas capillary waves need enough time to evolve so as to play a role in the breakup in the central cylindrical portion of the particle.

In order to completely understand the development of capillary waves on extended particle, Stone (1989) numerically investigated the problem of evolution of initial disturbance. They Fourier decomposed the surface with the isolation of the end pinching mechanism to understand the effect of each mode. They found that the capillary wave development near the central region of the particle was uniform in spite of the fact that the particle was of finite length and continually shortening due to the end pinching effect. This suggested that there was very little flow in the central region, and hence very little effect on the capillary wave dynamics due to continuous shortening of the particle near the ends except for very high viscosity ratio flows where the end-effects play an important role.

Figure 16 in Stone (1989) shows that the linear theory holds even though the disturbance is clearly finite amplitude. Very close to actual fragmentation, interface evolves more rapidly than theory predicts, which demonstrates that the nonlinear effects do eventually become noticeable, but only in the later stages of the breakup process in the cylindrical thread-like region (formation of satellite particles).

Non linear theory. Linear theory is correct up to the jet breakup but cannot predict all the sizes of the particles produced i.e it cannot predict the formation of satellite particles, which are in turn formed from the ligaments between the two main particles. A ligament can break into one or more satellite particles as observed in the experiments by Tjahjadi, Stone and Ottino (1992) (Figure 10). Pimbley and Lee (1977), Ashgriz and Mashayek (1995) and Rutland and Jameson (1970) have also done significant studies on the nonlinear theory and the formation of satellite particles and has been reviewed extensively in Ashgriz (2011).

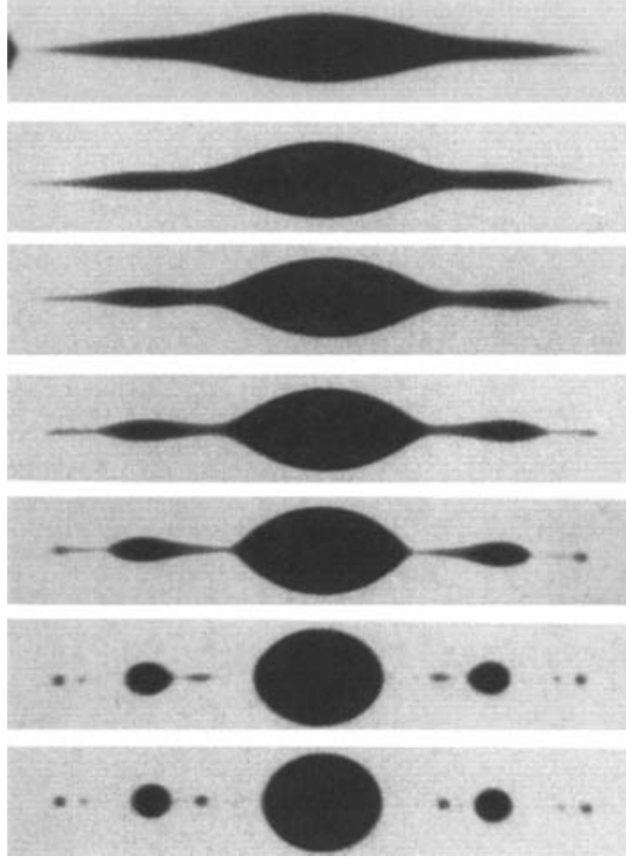


Figure 10: Experimental observation of the time evolution of ligament pinch-off from top (during first pinch-off) to bottom (during last pinch-off) at $\lambda = 0.067$ and $k = 0.45$. [Picture taken from Tjahjadi, Stone and Ottino (1992)].

Ashgriz and Mashayek (1995) calculated the size of the main daughter particle and the satellite particle for different wavenumbers as shown in the Figure 11. There was no significant change in both the main daughter particle and satellite particle size for $Oh < 1$.

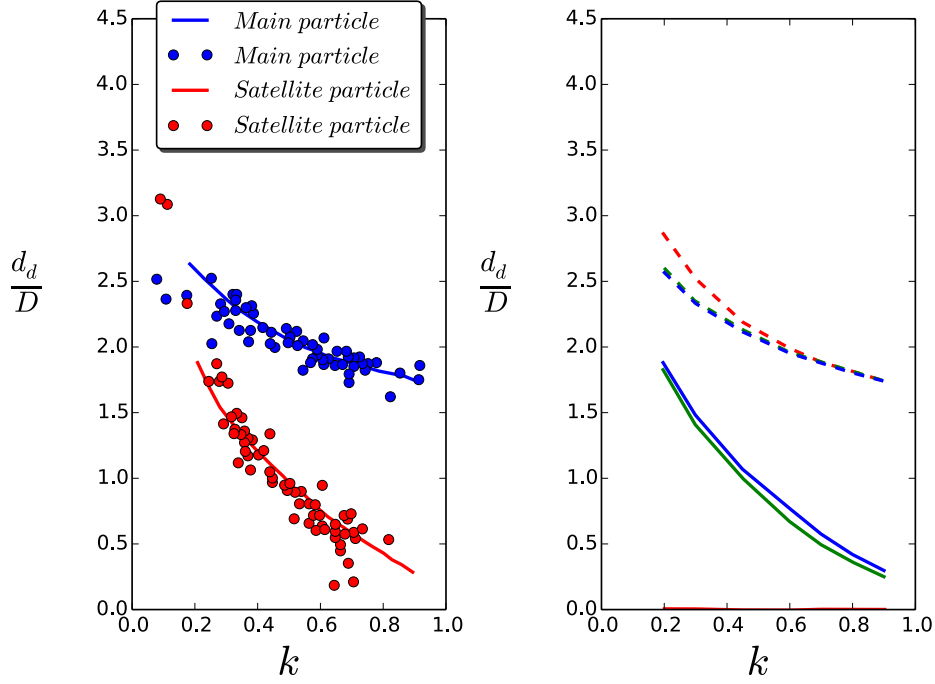


Figure 11: Left Figure: Variation of size of daughter particles (d_d =daughter particle diameter, D =jet diameter), Blue and Red dots: Experimental data of Rutland and Jameson (1970). Blue and Red lines: Non-linear theory of Ashgriz and Mashayek (1995). Right Figure: Effect of Ohnesorge number, Red dashed-line: Main particle size at $\frac{1}{Oh} = 0.1$, Green dashed-line: Main particle size at $\frac{1}{Oh} = 10$, Blue dashed-line: Main particle size at $\frac{1}{Oh} = 200$, Red solid-line: Satellite particle size at $\frac{1}{Oh} = 0.1$, Green solid-line: Satellite particle size at $\frac{1}{Oh} = 10$, Blue solid-line: Satellite particle size at $\frac{1}{Oh} = 200$. [Redrawn from Figure 8 in Ashgriz and Mashayek (1995)].

At higher values of Ohnesorge number ($Oh > 0.1$), size of the satellite particles is found to depend on the Oh value. Length and diameter of the ligament formed is found to decrease and consequently, the diameter of the satellite particles decreases at higher values of Oh and for very high values of Oh , satellite particles are not formed. They also found this limiting value of Oh for different values of k as shown in the Figure 12. Bousfield et al. (1986) also observed that the diameter of the satellite particles were larger than the main particle at very low values of k . Further, Spangler, Hibling and Heister (1995) studied the presence of aerodynamic effects on the nonlinear aspects of the jet and the sizes of the main daughter particles and the satellite particles.

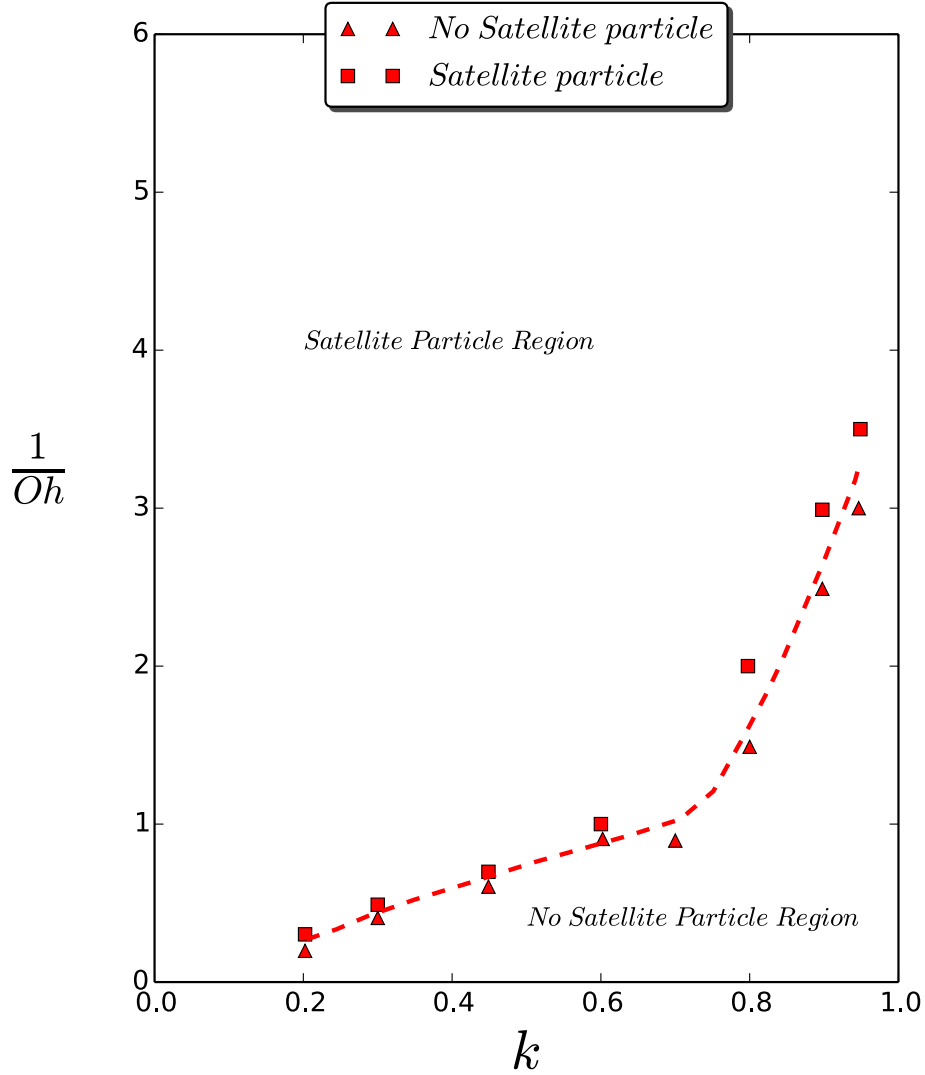


Figure 12: $Oh - k$ phase diagram denoting the Satellite particle and No Satellite particle region. [Redrawn from Figure 9 in Ashgriz and Mashayek (1995)].

Summarizing, linear capillary wave instability theory is not able to explain the existence or formation of satellite-particles, nor is it valid for the case when the disturbances reach finite amplitude (as observed during breakup). It implicitly assumes that all the disturbances are equally likely and the observed particle sizes after the breakup will correspond to the wavelength of the fastest growing linear mode. If the initial amplitude of this critical disturbance is known, then the time for breakup can be estimated. In addition, wavelength and growth rate of the critical disturbance depend on the viscosity ratio. For bubbles the inviscid limit is a good approximation, but for large viscosity ratios growth slows down. Whereas, nonlinear theory can explain the breakup of ligaments and the late stages of the breakup of jets, which in turn dictates the size of the satellite particles.

2.2.2. End pinching

Among the cases in which a particle was initially extended and then left free to observe its deformation, Stone (1986, 1989) found that there was no capillary waves during the elongation process or when the flow was on. There was also no such case wherein the extending particle fractured at the central region when the flow was on but the breakup was seen when the particle was left free. They observed that this breakup was due to the capillary pressure variations near the ends rather than the instability of the infinitesimal disturbances in particle shape and hence, named it as "end-pinching" mechanism.

For low viscosity particles, large interior velocity gradients are possible in the cylindrical region due to the pressure gradient unlike the high viscosity particles. This is the main cause for the end pinching mechanism.

When the low viscosity particles are subjected to pure straining flow, they develop long slender shapes with pointed ends. After the flow is turned off, the high initial curvature at the ends results in the large velocities near the ends and a very rapid reduction in the initial length. The initial pressure gradient drives the rapid relaxation and as the end becomes more spherical this pressure gradient diminishes. The pressure (due to the local curvature of the interface) also generates a local flow from the cylindrical region which thus causes a neck to form in the particle shape as illustrated in Figure 9 and also in the Figure 6 of Stone and Leal (1989).

Therefore, the mechanism for relaxation and breakup of an extended particle in an otherwise quiescent fluid consists of a competition between a pressure-driven flow near the end, which causes translation of the end toward the particle centre (thus tending to return the particle to its spherical equilibrium shape), and a pressure-driven flow away from the centre in the transition region which leads to the development of a neck and thus to breakup via a capillary pinch-off process.

Stone, Bentley and Leal (1986) also suggested that the final remnant parent particle size is determined by the rate at which ends bulb up and contract towards the particle centre, relative to the rate at which the ends pinch off. The timescale for this mechanism is much smaller than the growth of capillary waves.

Recently there have been few numerical studies (Li, Renardy and Renardy (2000), Renardy and Cristini (2001a,b) and Renardy, Cristini and Li (2002) using VOF, Komrakova et al. (2015) using diffuse interface free energy LBM) that observe the end pinching mechanism. Komrakova et al. (2015) observed end pinching mechanism at low shear rates and λ low values and observed capillary wave instability at low shear rates and high λ values.

2.2.3. Tip streaming and Tip dropping

Tip streaming and tip dropping are the modes of particle breakup that occur when surfactants are present. Taylor (1934) was the first to report the tip streaming phenomenon and he referred to it as a transient phenomenon since it disappeared when the shear rate was further increased. The true cause was identified by De Bruijn (1989, 1993). Janssen, Boon and Agterof (1994, 1997) were the first to observe the tip dropping phenomenon and also observed tip streaming in both simple shear flow and pure straining flows. For these breakup mechanisms in simple shear flows the particle develops a sigmoidal shape and a stream of

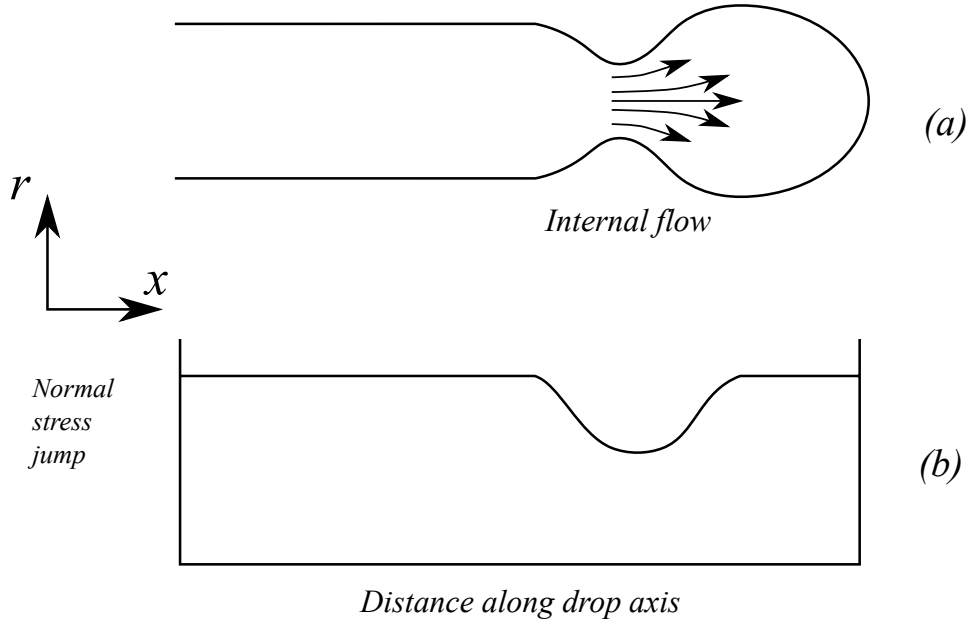


Figure 13: (a) Typical particle shape shortly after the flow is stopped. (b) Approximate normal stress jump across the interface.

tiny particles are ruptured off the tips of the parent particle as shown in Figure 14. This mechanism occurs for capillary numbers less than the critical value and it is important because the shear rates required for this type of breakup have in some circumstances been observed to be two orders of magnitude lower than that for the normal breakup (clean particle) in which the particle is broken in two or three almost equally sized particles with a few tiny satellite particles in between.

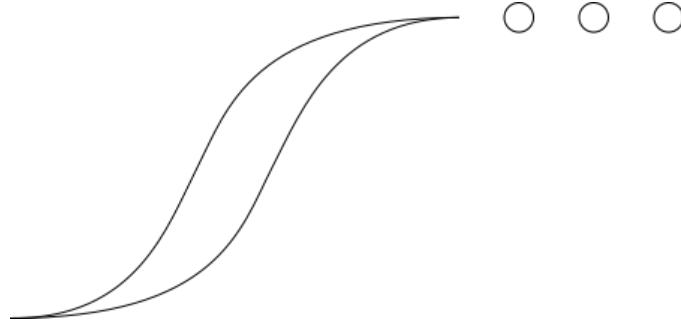


Figure 14: Graphical representation of Tip Streaming phenomenon.

According to De Bruijn (1989, 1993) tip streaming results from interfacial tension gradients with lower value at the tip and higher elsewhere. This phenomenon occurs when there is a moderate level of the surface active material. At lower levels of the surface active materials, surface tension is not low enough at the tip and at higher levels, surface tension is lowered uniformly and the gradients are too weak. Such interfacial tensions gradients

make the particle surface less mobile allowing the shear stresses exerted by the continuous phase to pull out a stream of tip particles. This explanation however can only hold good when the shear stresses exerted by the continuous phase are large enough to maintain such an interfacial tension gradient and when the diffusion of the surface active material from the particle to the surface is slow enough not to interfere with the buildup of the interfacial tension gradients.

De Bruijn (1989, 1993) experimentally determined the effect of various parameters on the tip streaming mechanism and found that it depends on the fluids used (doesn't seem to occur in all fluids) irrespective of the value of surface tension provided that the viscosity ratio is very less than one. They also found that this mechanism is some sort of depletion mechanism effect and depends on the history of the particle. The ruptured particle radii were two orders of magnitude smaller than their parent particle and had significantly reduced surface tensions.

Eggleton, Tsai and Stebe (2001) numerically simulated the particle breakup in linear uniaxial pure straining flow using a nonlinear model for the surface tension. They explained that the surface convection sweeps surfactants to the particle poles, where it accumulates and drives the surface tension to near zero. The particle assumes a transient shape with highly pointed tips. From these tips, thin liquid threads are pulled. Subsequently, small, surfactant-rich particles are emitted from the termini of these threads. After a finite number of daughter particles have been ejected, the cleaner parent particle can attain a stable shape. The scales of the shed particles are much smaller and depends on the initial surfactant coverage.

Dilute initial coverage leads to tip streaming, while high initial coverage leads to another mode of breakup called as tip dropping, wherein the daughter particles are larger and ejected more intermittently. The mechanism which causes the liquid threads to be pulled is same as that in the tip streaming phenomenon but due to the high initial surfactant coverage, larger liquid thread is pulled and the pinching takes place at the junction of the parent particle-thread as shown in Figure 15, which eventually forms a larger daughter particle.

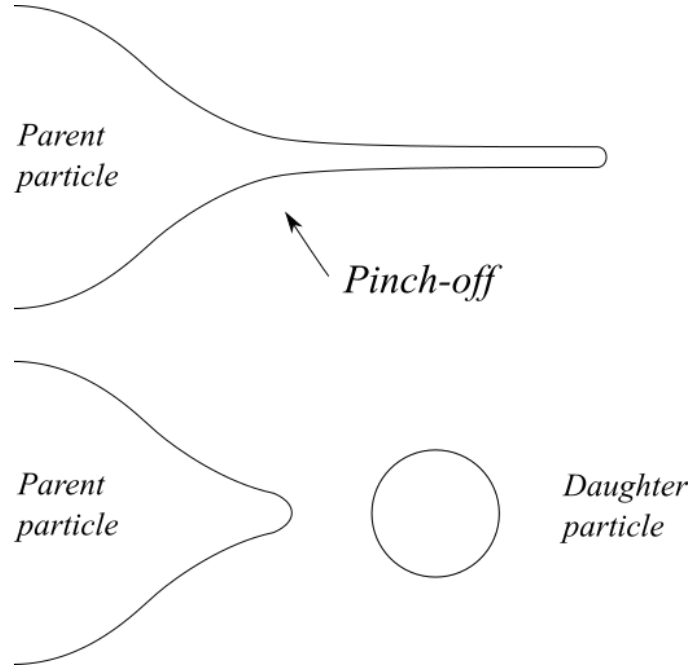


Figure 15: Graphical representation of Tip Dropping phenomenon.

Numerical simulations in Eggleton, Tsai and Stebe (2001) also showed that at trace surface concentrations, surface tension effects are negligible and the critical strain rate for a clean interface is reached before (Γ_∞ is approached at the pole. The particle becomes unstable and extends as a continuous thread, with the possibility of surfactants altering the breakup. At dilute concentrations convection drives the surfactants towards the pole and Γ_∞ is reached at strain rates below the critical strain rate for the clean particle. Surface tension at the pole approaches zero and sharp gradients in surface tension lead to the emission of a thread. Thread size increases with concentration. If significant surface tension gradients are present at high concentrations, the thread diameter will be comparable to the parent diameter, leading to particle fracture. Tip streaming occurs only when the $\lambda < 0.2$.

3. Inertial force driven breakup

As the Reynolds number increases, the Stokes flow approximation is no more valid and the inertial forces begin to dominate over the viscous forces. Hence, Weber number, Reynolds number, density ratio and viscosity ratio are the important parameters used to characterize the flow field. But depending on the viscosity, of the dispersed particles, Ohnesorge number is also considered for the study.

3.1. Straining flows

Miskis (1981) numerically calculated the steady particle shape in an axisymmetric pure straining flow in the limit of infinite Reynolds number using the boundary-integral technique. They found that there is no steady shape beyond a Weber number of value 2.76 which was

called a critical Weber number. They were the first to introduce this concept of critical Weber number. Later, Ryskin and Leal (1984) compared and extended the work of Miskis (1981) by considering the deformation of a particle in a uniaxial pure straining flow at finite Reynolds number values ($0.1 \leq Re \leq 100$). Critical Weber number was defined based on the observation of appearance of the waist and subsequent divergence of their numerical scheme signifying particle breakup. They also stated that the result provided by Miskis is accurate for $Re \geq 100$ and provided an interpolation formula for lower values of Reynolds number.

$$\left(\frac{1}{We_{crit}}\right)^{\frac{10}{9}} = \left(\frac{1}{2.76}\right)^{\frac{10}{9}} + \left(\frac{1}{0.247Re^{\frac{3}{4}}}\right)^{\frac{10}{9}} \quad (17)$$

They stated that the above case is only valid for bubble and not for inviscid drops and the two cases is identical only if the Reynolds number is zero or if the shape is fixed (spherical). Otherwise, one must take into account the variation of pressure inside the inviscid drop.

Kang and Leal (1987, 1989) studied the steady and unsteady deformation of a particle in a uniaxial and biaxial pure straining flow. They attempted to correlate the initial half-length $l_{1/2}$ with the critical Weber number (defined based on the steady state calculations) and observed (Figure 16) that it decreases as the initial elongation from steady shape increases and stated that the particle shape in a subcritical flow is stable in the neighborhood of steady state and unstable if sufficiently deformed at some initial instant as a consequence of stretching in a flow with $We < We_{crit}$. A limit point observed for the existence of steady axisymmetric particle shapes at a Weber number of $O(2-3)$ in uniaxial flow for all $Re \geq 10$ was not found for biaxial flow at any $We \leq O(10)$ for Re up to 200.

Other works on biaxial pure straining flows are Frankel and Acrivos (1970) who calculated particle shape in creeping flow limits to moderate values of capillary number ($Ca \leq 0.2$) and Hinze (1955), Lewis and Davidson (1982) at higher Reynolds number. Further uniaxial pure straining flow breakup is assumed to be a simplified model for breakup of particles in turbulent flows. Hence more studies on pure straining flows has been covered in the Section 4.2 (**Instantaneous breakup**).

3.2. Secondary breakup

Accelerating particles are found ubiquitous in the nature. Importance of these have been found in the wide range of applications ranging from rainfall in the nature to the spray atomization in combustion engines. Considering the vast research on this field and also accounting for the large number of existing reviews, a very brief account has been considered here.

When a particle breaks apart into a multitude of small fragments due to disruptive aerodynamic forces, the process is termed as secondary atomization. Pilch and Erdman (1987) defined the total breakup time as the time taken for a particle and its fragments to reach the steady state. Multiple correlations have been proposed and some are not in agreement with others refer Pilch and Erdman (1987), Hsiang and Faeth (1992), Gelfand (1996) and Gueldenbecher, Lopez-Rivera and Sojka (2006) for the correlations.

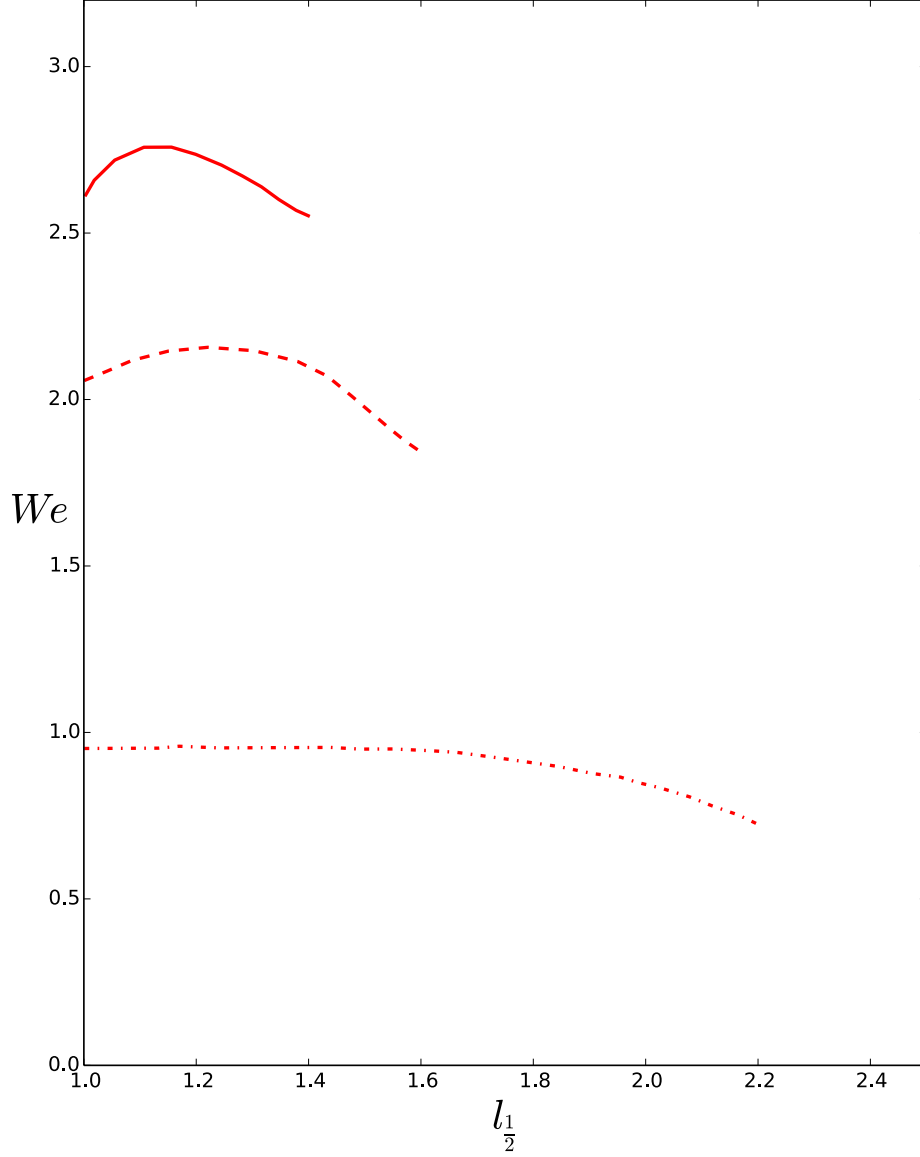


Figure 16: Effect of initial half-length of the particle $l_1/2$ on the critical Weber number. Solid line: $Re = \infty$, Dashed line: $Re = 100$, Dotted line: $Re = 10$ [Redrawn from Figure 7 in Kang and Leal (1987)].

The dominating forces that govern the breakup at high Reynolds number and high density ratio are aerodynamic forces which are counteracted by the restorative surface tension forces. The radical mode of breakup is found to be different for different magnitude of these competing forces. Hence the breakup mechanism is divided into different breakup regimes based on the range of aerodynamic Weber numbers (most important parameter for secondary atomization) as shown in the Table 1 at lower values of particle Ohnesorge

number and higher values of Reynolds number. At higher values of Ohnesorge number ($Oh > 0.1$), particle viscosity hinders deformation and also dissipates energy supplied by the aerodynamic forces, which reduces the tendency towards breakup, and hence was found to change the transitional We values to some extent. Many correlations are present for We_{crit} (weber number at which bag breakup starts) at high Oh but none is known to be accurate at $Oh > 1$. Reynolds number does not affect the breakup process, though at lower values, Aalburg, van Leer and Faeth (2003) has numerically observed significant change in transitional values. Han and Tryggvasson (1999, 2001) and Aalburg, van Leer and Faeth (2003) also observed that the critical Weber number increases as the density ratio reduces to 1 and is independent above 32.

Regime	We Range
Vibrational (no breakup)	$0 < We < \sim 11$
Bag breakup	$\sim 11 < We < \sim 35$
Multimode breakup	$\sim 35 < We < \sim 80$
Sheet thinning breakup	$\sim 80 < We < \sim 350$
Catastrophic breakup	$We > \sim 350$

Table 1: We for particles with $Oh < 0.1$ [Adapted from Guildenbecher, Lopez-Rivera and Soika (2006)].

3.2.1. Deformation and vibrational breakup

When a spherical particle enters the disruptive flow field, due to the higher static pressure at front and rear stagnation points when compared to the particle periphery, it deforms into an oblate spheroid. In some cases, the particle oscillates due to restoration by surface tension and this oscillation might lead to breakup. According to Pilch and Erdman (1987) this breakup mode does not lead to small final fragment sizes and the breakup time is long compared to other breakup modes.

3.2.2. Bag breakup

The We number at which the bag breakup starts is termed as the critical Weber number, $We_{crit} = 11 \pm 2$ (Guildenbecher 2009). In this mode of breakup, a bag is formed due to the pressure difference between the leading stagnation point and the wake of the particle (Han and Tryggvason 1999, 2001), though the exact reason for the formation of bag is still an open question. The outer edge forms a toroidal ring to which the bag is attached (Figure 18a). Chou and Faeth (1998) also reported that bag breakage results in larger number of small fragments (average size 4% of parent particle), whereas the toroidal ring into smaller number of large fragments (average size 30% of parent particle).

Chou and Faeth (1998) studied the temporal characteristics of this breakup and showed that it requires $5 \sim 6$ characteristic timescale t_c for complete breakup, where t_c is given by,

$$t_c = \frac{D_0 \left(\frac{\rho_d}{\rho_c} \right)^{\frac{1}{2}}}{U} \quad (18)$$

3.2.3. Multimode breakup/ transition or chaotic breakup

It is a combination of two breakup modes or can be considered as a transition between two breakup modes. As seen in the Figure 17, it is accompanied by a bag and a long filament at the center, which is also referred as plume/stamen (Pilch and Erdman 1987). It can also be a combination of bag and sheet-thinning breakup (Dai and Faeth 2001) or a multi-bag breakup (Cao et al. 2007) (Figure 18c).



Figure 17: Multimode breakup [Picture taken from Guildenbecher and Sojka (2011)].

Rayleigh-Taylor instability was thought to be the mechanism behind this breakup along with the aerodynamic intensification effects and hence was called a combined "Rayleigh-Taylor/aerodynamic drag" mechanism (Jain et al. 2015, Jain et al. 2016, 2017).

3.2.4. Sheet-thinning breakup

According to Liu and Reitz (1997), at higher We numbers a sheet is formed at the deflected periphery of the particle which evolves into ligaments that break up into multiple fragments. This process continues until the particle is completely fragmented or until it has accelerated to the point at which aerodynamic forces are negligible and finally a core particle remains at the end (Figure 18d). This process was mistakenly assumed to be due to the shear from the continuous phase flow over the deformed particle which results in the formation of the boundary layer inside the particle surface and this boundary layer becomes unstable at the periphery resulting in the stripping of mass and hence was previously called as Shear Stripping (Ranger and Nicholls 1969).

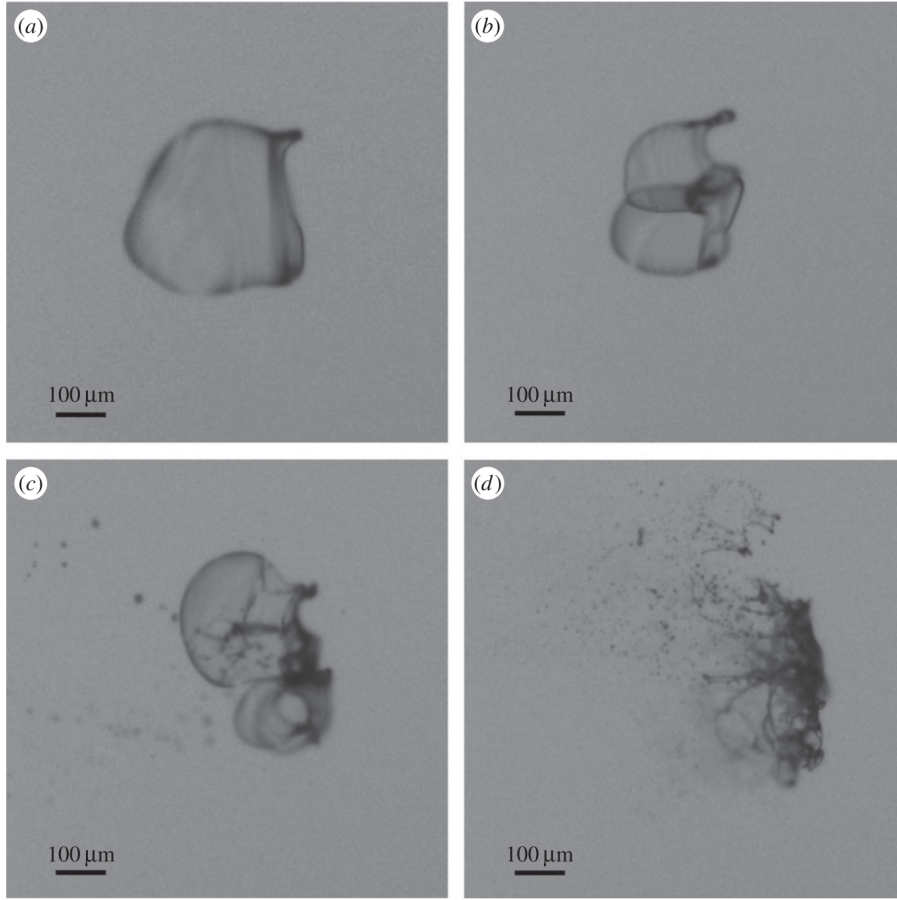


Figure 18: Secondary breakup of particles. (a) $We = 20$ (bag breakup), (b) $We = 40$ (bag-stamen breakup), (c) $We = 80$ (multi-bag breakup) and (d) $We = 120$ (sheet-thinning breakup). [Picture taken from Jain et al. (2015)].

3.2.5. Catastrophic Breakup/piercing breakup

At very high We numbers, unstable surface waves have been observed on the leading edge of the particle, which eventually penetrates into the particle causing multiple fragment breakup. Liu and Reitz (1993) considered this phenomenon to be a result of Rayleigh-Taylor instability due to the acceleration of lighter medium towards the denser medium. Though, most experimental observations show the formation of waves on the front end of the particles, there has been few speculations on the occurrence of the waves on the rear end of the particles.

Recently there have been few numerical studies of secondary breakup. Works that study secondary breakup at low density ratios ($\frac{\rho_d}{\rho_c} < 100$) are Kkesi, Amberg and Wittberg (2014), Han and Tryggvason (1999) and at high density ratios by Xiao, Dianat and McGuirk (2014) and Jain et al. (2015). Renardy (2008) and Kkesi (2016) studied the breakup when both the inertia and viscous forces are considerable i.e., inertial breakup with shear. Renardy

(2008) studied the inertial breakup of a particle in an initially established shearing external fluid at subcritical capillary numbers. They observed that the particle extended more than when it was placed in a gradually increasing shearing external fluid before it broke. Kkesi 2016 in their numerical simulations observed 5 different modes (bag, shear, jellyfish shear, thick rim shear, thick rim bag) of breakup in the presence of inertia and shear. Increasing the Reynolds number, shear rate and decreasing viscosity ratio they observed the breakup mode tending towards the shearing breakup.

At very low density ratios, transitional We has not been found to match with the experiments. Hence in a recent study by Jain et al. (2016, 2017), the effect of density ratio on the breakup was studied and it was found that there exists a critical density ratio value below which the dynamics is different from that at the higher values (observed in experiments). Though most of the numerical and experimental studies try to understand the mechanism behind the different breakup modes, a good agreement between the different studies has not been achieved yet and hence there is a huge scope for better and more detailed numerical and experimental studies.

3.3. Breakup under the action of gravity in stagnant media

Particles under the action of gravity involves freely rising or falling particles in a stagnant medium. The breakup mechanism in this situation is explained as follows: the breakup can only occur if the disturbance located at the advancing front of the particle grows quickly enough and reaches sufficient amplitude before being swept around the equator. Ryskin and Leal (1984) compared the deformation of a rising particle in quiescent fluid to the pure straining flow and stated that the phenomenon is much simpler in case of pure straining flow. In the case of rising particle, unlike the pure straining flow, capillary number does not play a role even at the low Reynolds numbers. Though, the Weber number does determine the deformation at non-zero Reynolds numbers, the deformation is rather small at $We = O(1)$, and, indeed extremely high Weber numbers can be reached experimentally for spherical-cap particles without breakup, the shape of a particle becoming essentially independent of We above some value of order 15-20. Hence neither Ca or We can be a direct measure of the strength of the dominant deforming force relative to the restoring tendency of the surface tension.

Earliest experimental work on the breakup of particles freely moving under the action of gravity in liquid-liquid systems can be found in Hu and Kinter (1955). Klett (1971), Ryan (1978) analyzed liquid drops falling in air. Other works which focused on bubbles are Clift and Grace (1973), Clift, Grace and Weber (1974). Krishna, Venkateswarlu and Narasimhamurty (1959), correlated the maximum size of a liquid drop falling in water.

$$d_{max} = \frac{2.25U_M^2}{g(\rho_d - \rho_c)} \text{ in cm} \quad (19)$$

where U_M is in cm/s and is given by,

$$U_M = \frac{0.568\sigma}{\mu_c S_d^{1.305}} \quad (20)$$

and S_d is given by,

$$S_d = \frac{g_c \sigma}{\mu} \left(\frac{3}{4g} * \frac{\rho^2}{\mu_c \Delta \rho} \right)^{1.3} \quad (21)$$

where g_c is equal to $980.6 \text{ (mass)(cm.)/(gramsforce)(sec}^2\text{)}$ and g is $978 \text{ grams per cm.}$ Here σ is expressed in *dynes per cm*, ρ_c and ρ_d in *grams per ml* and μ_c in *grams per cm. sec.*

According to Komobayasi, Gonda and Isono (1964), average life time of water drop suspended in a vertical air stream depends on the drop diameter. They obtained an empirical formula,

$$t_b = 3.4 \times 10^6 e^{-17D} \quad (22)$$

where d is expressed in cm and t_b is the life time of the drop before it breaks in *seconds*. They also said that the number of droplet fragments produced depends on the diameter of the drop and obtained an empirical relation for the size distribution,

$$N(d_d)\delta(d_d) = 6.25 \times 10^{-2} d_p^3 e^{-7.8D} \delta d_d \quad (23)$$

where d_d and d_p are expressed in *cm*.

Since there is no direct measure of any non-dimensional number for the breakup in the case of free-fall or free-rise, other factors involved such as surface instability and the dependence on the initial shape are further considered.

3.3.1. Surface instabilities

The breakup of particles under the action of gravity is assumed to be due to surface instabilities. Hence considerable amount of research has been done to study the effect of surface instability on the bubbles and drops. Accordingly, there exists a maximum particle size above which the particle succumbs to breakup due to surface instability. The maximum stable bubble size is of the order of several *cm*. Clift, Grace and Weber (1978, ch 12.III p. 341) quote a value of $\sim 49 \text{ mm}$ for air bubbles in water. Grace, Wairegi and Brophy (1978) have experimentally determined values between 45 and 90 *mm* for air bubbles rising in otherwise stagnant viscous media.

Different instability mechanisms have been proposed as an explanation. The Rayleigh Taylor instability has been considered by Grace, Wairegi and Brophy (1978) to derive a lower bound for the maximum stable particle size as,

$$d_{max} = 4 \sqrt{\frac{\sigma}{g(\rho_l - \rho_g)}} \quad (24)$$

For drops ($\lambda \geq 0.5$) the data they have compiled show good agreement with this value (see

also Clift, Grace and Weber 1978, ch 12.III p 341), but for bubbles the observed maximum stable bubble sizes are about a factor of ~ 10 larger.

A more refined treatment of the Rayleigh-Taylor instability has been given by Batchelor (1987) taking into account the stabilizing effect of the liquid acceleration along the particle surface. The Kelvin-Helmholtz instability has been considered in (Kitscha 1989) and (Wilkinson 1990). Centrifugal forces due to the internal circulation modify the simple treatment of instabilities above. These have been considered on a phenomenological basis in (Levich 1962) and (Luo 1999).

3.3.2. *Dependence on initial shape*

Final shape and state of the particles freely rising in stagnant media have been found to depend on the initial shape of the particle. Bhaga and Weber (1981) with the help of experiments characterized the shape of the particle freely rising in gravity as shown in the Figure 19.

More recently, Ohta et al. (2005) studied the effect of initial shape on the motion and final state of rising particle for which they did a computational study using coupled level-set / volume-of fluid method. They studied the final shape of the particle for different initial shapes in “spherical cap” regime. According to their observation, the particle breaks into a toroidal particle if it is spherical initially, whereas an initially spherical cap particle retains its shape as shown in the Figure 20. But the terminal velocity is found to be independent of the initial shape and for particles from regimes other than “spherical cap”, the final shape of the particle is found to be independent of the initial shape.

Another important observation was the breakup of spherical particles in toroidal particles, which was further numerically studied by Bonometti and Magnaudet (2006). They produced a phase plot [Bond number vs Archimedes number] as shown in Figure 21, indicating the transition from the spherical cap regime to toroidal particle regime for the particles with initially spherical shape and rising freely under the action of gravity.

Very recently, Tripathi, Sahu and Govindarajan (2015) extended this study to present a complete phase plot of all the regimes for an initially spherical particle rising freely under gravity. Brief of what was presented by them is included in Figure 22.

Hence an air bubble of diameter as low as 6mm is found to breakup in water which is contradicting to what was observed by Grace, Wairegi and Brophy (1978). Observations on dependence of the initial shape made by Ohta et al. (2005) explains the missing link for the stability of high diameter bubbles observed by Grace, Wairegi and Brophy (1978), wherein the experiments were done with initial spherical cap shape for bubbles. Hence a bubble remains stable even above the critical diameter given by Grace, Wairegi and Brophy (1978) if its initial shape is a spherical cap.

4. Breakup in complex Turbulent flows

Turbulent flows are the most complex and highly unsteady flows of all types. Considering its application range, present day research mostly deals with turbulent flows.

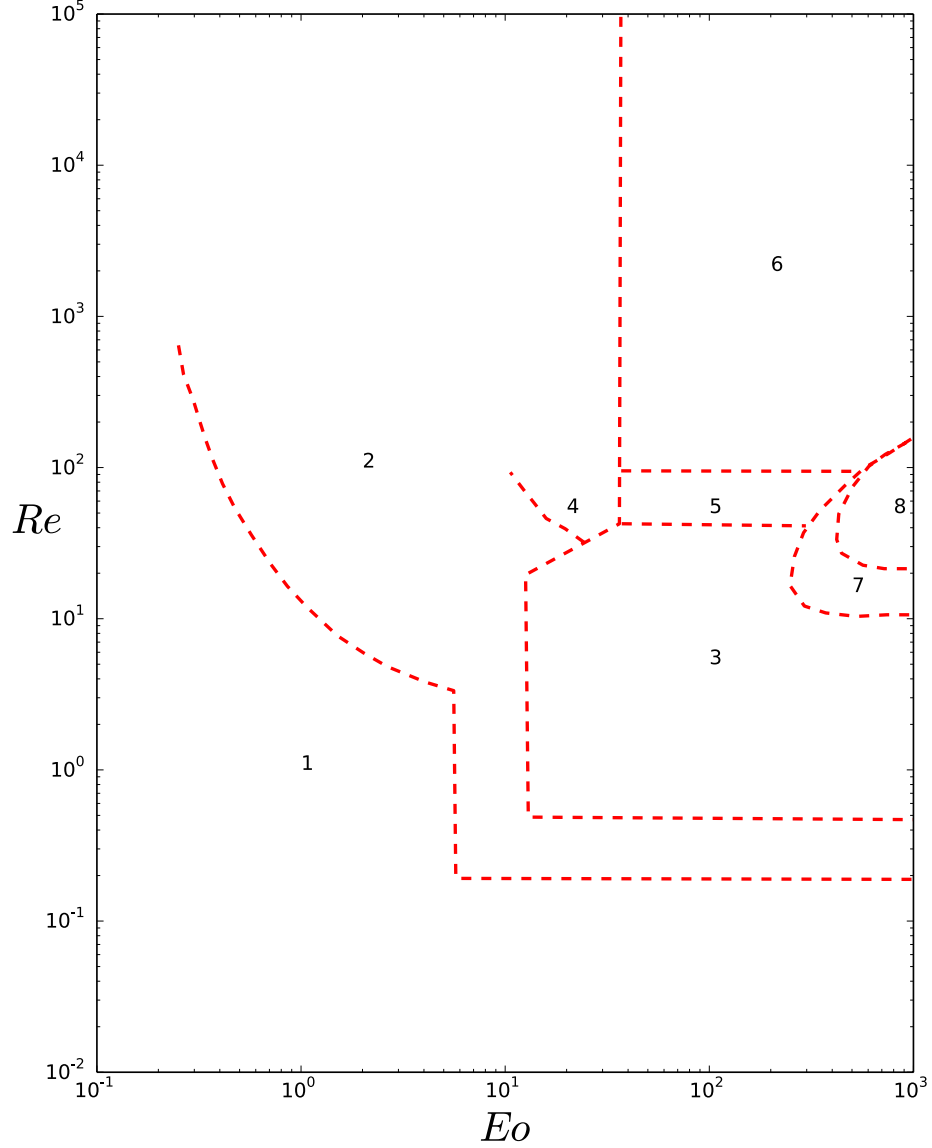


Figure 19: Shapes of freely rising particle in different regimes. 1: spherical, 2: oblate ellipsoid, 3: oblate ellipsoidal cap, 4: oblate ellipsoidal (disk-like and wobbling), 5: spherical cap with closed, steady wake, 6: spherical cap with open, unsteady wake, 7: skirted with smooth, steady skirt, 8: skirted with wavy, unsteady skirt [Redrawn from Figure 8 in Bhaga and Weber (1981)].

4.1. Basic concepts

Hinze (1955) was the first to provide a classification based on the shape of the breakup of particles in turbulent flows into three kinds, i.e. lenticular, cigar shape and bulgy. A universal frame work based on static force balance was designed, according to which the

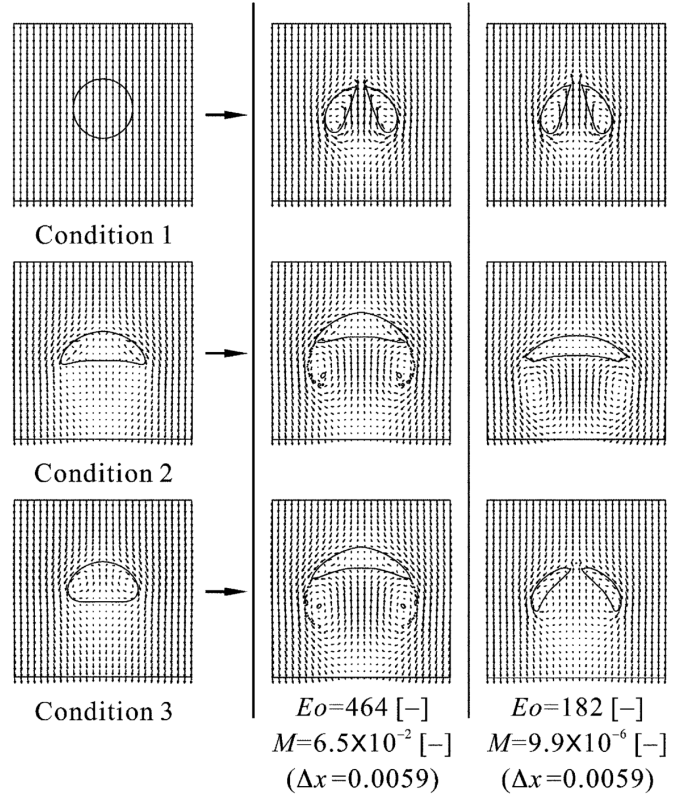


Figure 20: Particle rise depending on initial shape for spherical-cap regime. Condition 1: initially spherical particle, Condition 2 & 3: initially deformed particles [Picture taken from Ohta et al. (2005)].

deformation of a particle is due to the external force which is counteracted by the surface tension that tends to restore the sphericity of the particle. Few assumptions were made to complement this theory: 1. Particles are larger than the Kolmogorov length scale and hence the inertial effects dominate over the viscous ones. 2. Only velocity fluctuations close to the particle diameter are capable of causing large deformation. This theory was independently developed by Komogorov (1949) and Hinze (1955) and hence it is referred to as Kolmogorov-Hinze Theory.

Weber number is defined in terms of turbulent stress as,

$$We = \frac{\tau d}{\sigma} \quad (25)$$

According to the theory, further substituting the turbulent stress $\tau = \overline{\rho_c u'^2}$ and the velocity fluctuation over a scale of the size of the particle for homogeneous isotropic turbulence $\overline{u'^2} = C_2 d)^{\frac{2}{3}}$ gives (Batchelor 1951, ch 6.5),

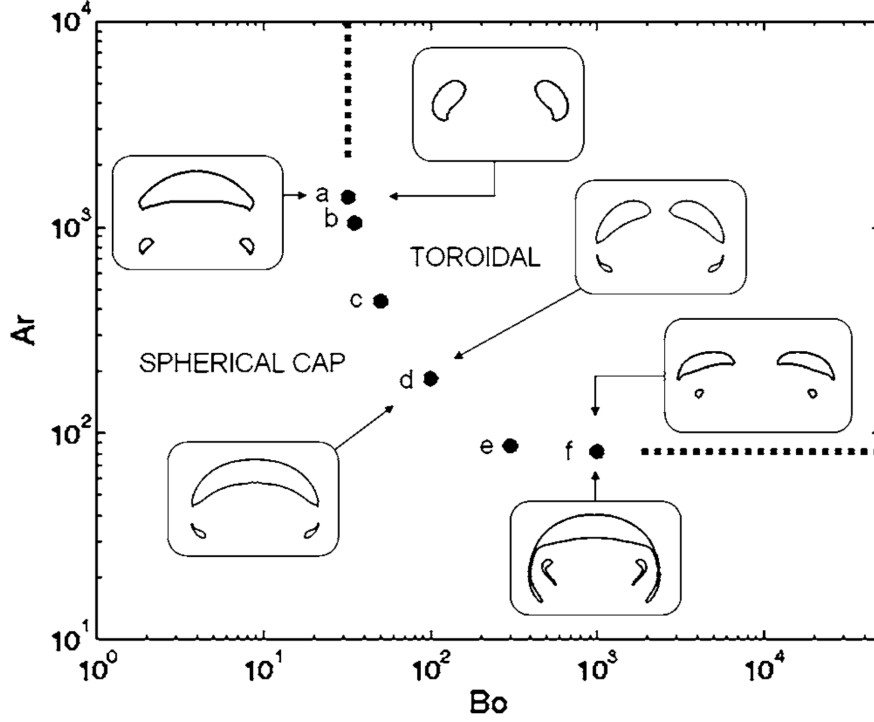


Figure 21: Transition from spherical cap particles to toroidal particles. Particle shapes are those observed just below and above the transition line. Vertical and horizontal dashed lines indicate the location of the transition for the inviscid regime ($Ar = \infty$) and the purely viscous regime ($Bo = \infty$), respectively [Picture taken from Bonometti and Magnaudet (2006)].

$$We = \frac{C_2 \rho_c \varepsilon^{2/3} d^{5/3}}{\sigma} \quad (26)$$

A critical diameter d_{max} is defined based on the critical value of the Weber number We_{crit} at which the breakup occurs, which was also used by Shinnar (1961):

$$d_{max} = We_{crit} \left(\frac{C_2 \rho_c}{\sigma} \right)^{-3/5} \varepsilon^{-2/5} \quad (27)$$

A similar theory on force balance was proposed by Levich (1962), wherein the internal pressure of the particle is balanced with the capillary pressure of the deformed particle. The contribution of the particle density is included through the internal pressure force term. Hence,

$$We = \frac{\tau d}{\sigma} \left(\frac{\rho_d}{\rho_c} \right)^{1/3} \quad (28)$$

Risso and Fabre (1998) and Delichatsios (1975) criticized the model for using of average

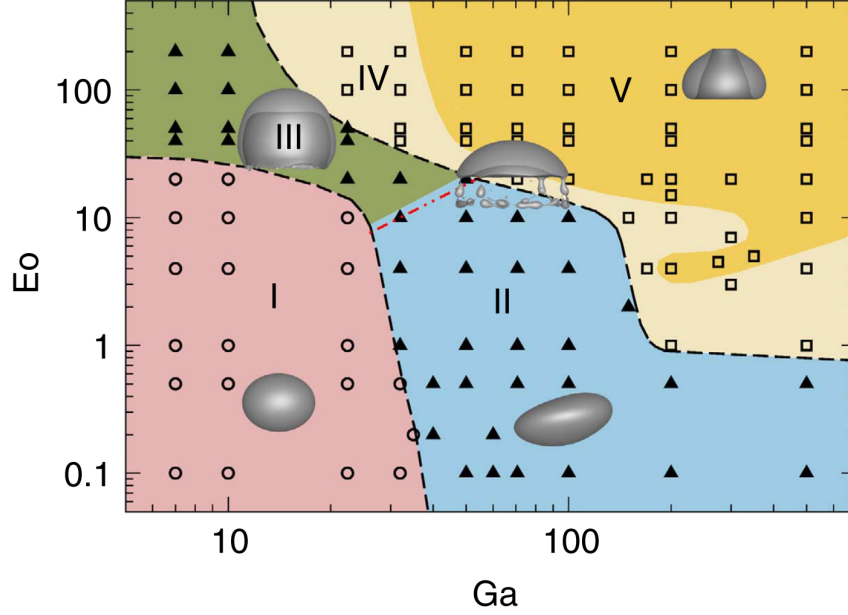


Figure 22: Initially spherical particle rising freely in different regimes. Region I: ellipsoidal in shape, axisymmetric, takes on terminal velocity. Region II: deviates from axisymmetry, shapes change with time. Region III: axisymmetric with thin skirt, attain terminal velocity. Region IV: axisymmetric upto breakup, spherical cap, peripheral breakup, axisymmetry after breakup, finally reaches terminal velocity. Region V: doughnut or toroidal shape, small satellite particles near the boundary, breaks into multiple particle fragments due to instability. In region IV, for high M , wide skirt was formed which broke off into small particle, for medium M , small particles were ejected from rim, for low M , narrow skirt resulting in ellipsoid rather than cap like particle. They used Eo with radius of the particle as the length scale [Picture taken from Tripathi, Sahu and Govindarajan (2015)].

value of velocity fluctuations rather than max value. Risso and Fabre (1998), Kang and Leal (1990) and Sevik and Park (1973) also noticed that the model neglects transient effects like resonance of accumulation of deformation.

Walter and Blanch (1986) was one of the early works to describe the processes involved in the particle breakup. With the help of high-speed videos, they observed single particle breakup and suggested that the breakup is essentially a three step process: (i) oscillation (ii) stretching into a dumbbell shape (iii) pinching off. They gave an expression for critical diameter, which was also confirmed by Hesketh, Russell and Etchells (1987) and Hesketh, Etchells and Russell (1991a, 1991b):

$$d_{max} = 1.12 \frac{\sigma^{0.6}}{\left(\frac{P}{V}\right)^{0.4} \rho^{0.2}} \left(\frac{\mu_c}{\mu_d}\right)^{0.1} \quad (29)$$

Various correlations have been derived by other authors and are listed in the Table 2 along with the flow conditions considered.

Table 2: Correlations for critical diameter derived for various flow conditions.

Author	Max diameter	Flow conditions
Hinze (1955), Shinnar (1961)	$d_{max} = We_{crit} \left(\frac{C_3 \rho_c}{\sigma} \right)^{-\frac{3}{5}} \varepsilon^{-\frac{2}{5}},$ where $C_3 = \text{contant}$	Particles with viscosity ratio $\lambda = 1$
Sleicher (1962)	$\frac{d_{max} \rho_c V^2}{\sigma} \sqrt{\frac{\mu_c V}{\sigma}} = C_4 \left[1 + 0.7 \left(\frac{\mu_d V}{\sigma} \right)^{0.7} \right]$ $C_4 = 38$ with 1.5 inch I.D of pipe.	Drops of two immiscible liquids in turbulent pipe flow
Paul (1965)	$\frac{d_{max} \rho_c V^2}{\sigma} \sqrt{\frac{\mu_c V}{\sigma}} = C_5 \left[1 + 0.7 \left(\frac{\mu_d V}{\sigma} \right)^{0.7} \right]$ $C_5 = 43$ with 1.5 inch I.D of pipe. C_5 is dependent on the pipe diameter.	Drops of two immiscible liquids in turbulent pipe flow
Wallis (1969)	$d_{max} = 0.752 \sigma^{0.6} \varepsilon^{-0.4} \rho^{-0.2}$	Particle in liquid
Kubie and Gardner (1977)	$\left[\frac{d_{max} \rho_c u^2}{\sigma} \right] \left[\frac{f d_{max}}{D} \right]^{\frac{2}{3}} = 0.369$ $f = 0.076 Re^{-0.25}$ for straight pipe $f = 0.076 Re^{-0.25} + 0.00725 \left(\frac{D}{D_H} \right)^{0.5}$ for helix pipe	Drops of liquid-liquid system in pipe flow
Arai et al. (1977)	$\frac{d_{max}}{D_i} = C_6 \cdot \left(\frac{\rho_c n_r D_i^2}{\mu_d} \right)^{-0.75}$ when dispersed phase viscosity μ_d is not negligible considerable	Particles in mixing vessel
Lewis and Davidson (1982)	$d_{max} = 1.67 \sigma^{0.6} \varepsilon^{-0.4} \rho^{-0.2}$ Industrial bubble columns ($\varepsilon \approx 1 kW/m^3$) - $d_{max} = 5.5 mm$, Laboratory stirred tank ($\varepsilon \approx 10 kW/m^3$) - $d_{max} = 2.2 mm$	Rising gas bubbles in a liquid jet flowing upwards through a large volume of the same liquid
Davies (1985)	$d_{max} = C_7 * \left(\sigma + \frac{\mu_d u'}{4} \right)^{0.6} \rho_c^{-0.6} \varepsilon^{-0.4}$	Particle in liquid emulsions
Walter and Blanch (1986)	$d_{max} = 1.12 \frac{\sigma^{0.6}}{\left(\frac{P}{V} \right)^{0.4} \rho^{0.2}} \left(\frac{\mu_c}{\mu_d} \right)^{0.1}$	Particles in turbulent pipe flow
Calabrese, Wang and Bryner (1986), Sathyagal, Ramkrishna and Narsimhan (1996)	$\frac{d_{32}}{d_{o32}} = 0.053 We^{-0.6} (1 + 4.42 Oh)^{3/5}$ where $Oh = \frac{\sqrt{\frac{\rho_c}{\rho_d}} \mu_d \varepsilon^{-\frac{1}{3}}}{\sigma} d_{32}^{\frac{1}{3}}$ as $Oh \rightarrow 0$ $\frac{d_{32}}{d_{o32}} = 0.053 We^{-0.6}$ as $Oh \rightarrow \infty$ $\frac{d_{32}}{d_{o32}} = 0.13 \left(\frac{\rho_c}{\rho_d} \right)^{\frac{3}{8}} \left(\frac{\mu_d}{\mu_c} \right)^{\frac{3}{4}} Re^{-\frac{3}{4}}$ and $\frac{d_{32}}{d_{max}} = 0.48$ to 0.6 depending on the value of the μ_d	Particles in turbulent stirred tanks
Hesketh (1987)	$d_{max} = \left(\frac{We_{crit}}{2} \right)^{0.6} \left[\sigma^{0.6} / (\rho_c^2 \rho_d)^{0.2} \right] \varepsilon^{-0.4}$ with $We_{crit} = 1.1$	Bubbles in liquids in horizontal pipelines

The shape of the particles proposed by Hinze (1955) was experimentally verified by Risso and Fabre (1998). Their experiments were performed in microgravity to minimize the bulk motion of the particle. They defined a parameter, A^* - (Relative difference of the projected area with respect to that of sphere - Equation 30) and performed experiments to study the relation between the maximum projected area A_{\max}^* and the percentage of breakup and found that there was no breakup for A_{\max}^* less than 0.5, 75% breakup for A_{\max}^* between 0.5 and 1 and 100% breakup for A_{\max}^* greater than 1. Hence they proved that the particles were significantly lengthened before they broke.

$$A^* = \frac{4A}{\pi d^2} - 1 \quad (30)$$

Number of fragments formed in a particle breakup was also observed by Risso and Fabre (1998). They observed that the majority of the breakup was binary:

1. 2 fragments (48%).
2. 3-10 fragments (37%).
3. >10 fragments (15%).

Further breakup can be classified into 2 cases: instantaneous breakup and resonance breakup. Though the resonance breakup was not a part of Kolmogorov-Hinze theory initially, it was included by Risso and Fabre (1998). Hence further detailed focus lies in these breakup processes.

4.2. *Instantaneous breakup*

When the weber number of the flow is greater than the critical Weber number, the sudden breakup without any significant previous deformation is said to be an instantaneous breakup. This type of instantaneous breakup was experimentally observed by Risso and Fabre (1998) and numerically modelled by Higuera (2004), Revuelta, Rodriguez-Rodriguez and Martinez-Bazan (2006), Rodriguez-Rodriguez, Gordillo and Martinez-Bazan (2006), Galinat et al. (2006), Revuelta (2010) and Padrino and Joseph (2011). Notable characteristics of this breakup process are:

- This breakup is independent of the turbulence history.
- The breakup might be either into two parts or many fragments.
- Breakup is only due to a single eddy.
- Second Eigen mode of the oscillation is largely predominant.
- The breakup process is approximately axisymmetric.
- Breakup is caused by the turbulent eddies of the same size as that of the particle.

- The flow outside the particle can be assumed to be steady since the characteristic turnover time t_t of a turbulent eddy is larger than the breakup time t_b .
- Breakup is uniaxial, and hence an initially round particle is stretched along a preferential direction until it breaks. This was inferred from the study of a biaxial breakup of a particle, which resulted in forming a disk followed by a torus and the breakup time was found to be larger than the uniaxial flow.

Critical weber number values have been experimentally and numerically determined by various authors for various flow conditions. They are listed in the Table 4.

Uniaxial Straining Force (USF) Model. Following the idea of static force balance, Martinez-Bazan, Montanes and Lasheras (1999) developed an empirical model for breakup frequency at high Reynolds number and Weber number, based on the difference between the turbulent stress and the surface stress.

for $Re \rightarrow \infty$

$$t_b \approx \left(1 - \frac{We_{crit}}{We}\right)^{-\frac{1}{2}} \quad (31)$$

$$g^* \approx \left(1 - \frac{We_{crit}}{We}\right)^{\frac{1}{2}} \quad (32)$$

Where g^* is equal to dimensionless breakup frequency. This was validated recently by Padrino and Joseph (2011), who used a Boundary element method to perform a viscous irrotational analysis. This model has been widely accepted and is being used as the breakup model for turbulent flows in most of the commercial and open source CFD solvers.

Further, Revuelta, Rodriguez-Rodriguez and Martinez-Bazan (2006) extended the model for finite Re values using a level-set numerical scheme. They analyzed the influence of the steady, axisymmetric pure straining flow on a particle and found that the critical value of We is 2.2 for $Re \geq 20$ and that the breakup time was significantly different for finite Reynolds numbers as shown in the Figure 18. Finally, they included the effect of Reynolds number in the expression of the breakup frequency.

$$t_b \approx \left(1 + \frac{15.5}{Re}\right) \left(1 - \frac{We_{crit}}{We}\right)^{-\frac{1}{2}} \quad (33)$$

Effective size range:. Though it was presumed that the breakup is caused by turbulent eddies of same size, Higuera (2004) went on to numerically study the collision of an axisymmetric stationary particle with a vortex ring of varying sizes to further explore the behavior of the breakup. Vortex ring was assumed to be an approximation for a turbulent eddy, though

Table 4: Critical Weber numbers for various flow conditions.

Author	Critical Weber number	Flow conditions
Hinze (1955)	$We_{crit} \approx 1.2$	Particles with viscosity ratio $\lambda = 1$.
Sevik and Park (1973)	$We_{crit} \approx 2.6$	Air bubbles in turbulent water jet.
Miskisis (1981)	$We_{crit} \approx 2.76$	Particles in steady axisymmetric pure straining flow (a simplified approximation to turbulent instantaneous breakup)
Lewis and Davidson (1982)	$We_{crit} \approx 4.7$	Rising gas bubbles in a liquid jet flowing upwards through a large volume of the same liquid.
Ryskin and Leal (1984)	$\left(\frac{1}{We_{crit}}\right)^{\frac{10}{9}} = \left(\frac{1}{2.76}\right)^{\frac{10}{9}} + \left(\frac{1}{0.247Re^{\frac{3}{4}}}\right)^{\frac{10}{9}}$	Particles in steady axisymmetric pure straining flow (a simplified approximation to turbulent instantaneous breakup)
Walter and Blanch (1986)	$We_{crit} \approx 2.4$	Particles in turbulent pipe flow.
Hesketh, Russell and Etchells (1987)	$We_{crit} \approx 1$	Bubbles in liquid in horizontal pipelines.
Kang and Leal (1987)	$We_{crit}(Re) = 1.8(10), 4.2(100), 5.4(\infty)$	
Risso and Fabre (1998)	$We_{crit} = 2.7 \sim 2.8$	Particles in microgravity condition.
Revuelta, Rodriguez-Rodriguez and Martinez-Bazan (2006)	$We_{crit} = 2.2$ for $Re \geq 20$	Numerically calculated using USF (Uniaxial Straining Force) model.

they knew that it is far from realistic collisions, they tried to make a qualitative study. They found that,

- For $R_{vp} < 0.75$, breakup was into 2 daughter particles of approximately same size.
- For $0.75 < R_{vp} < 1.1$, particle tears off.
- For $R_{vp} > 1.1$, a hole is punched at the symmetry axis, which transforms the particle into an elongated torus.

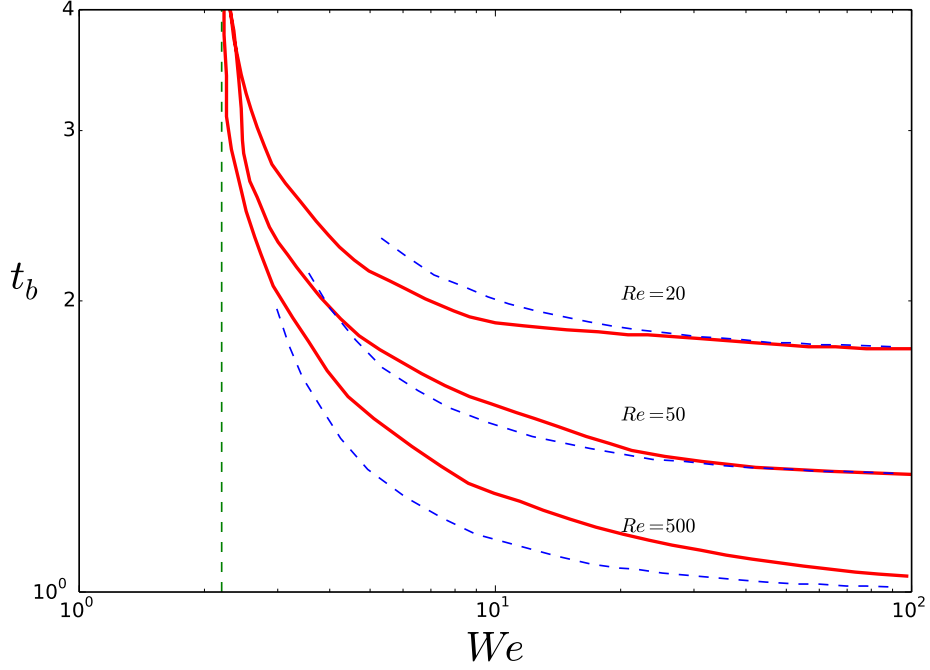


Figure 23: Dependence of breakup time t_b of a particle on the weber number We and Reynolds number Re for supercritical Weber number. Solid lines: results obtained by Revuelta, Rodriguez-Rodriguez and Martinez-Bazan (2006). Dashed blue lines: approximated relation in Eq. (30). Dashed green line: critical Weber number [Redrawn from Figure 5 in Revuelta, Rodriguez-Rodriguez and Martinez-Bazan (2006)].

where R_{vp} is the ratio of the radius of the vortex ring to that of the particle. Finally correlating the translatory velocity with the velocity scale at inertial range of turbulent flow, they arrived at the expression,

$$We = We_b R_{vp}^{\frac{2}{3}} \quad (34)$$

where $We_b \sim \frac{\rho \varepsilon^{\frac{2}{3}} a^{\frac{5}{3}}}{\sigma}$ is the Weber number for vortices of radius equal to that of the particle. Intersection of the plot of this weber number with that of the critical weber number gives a range for the radius of the vortex which is effective in breaking the particle. Rodriguez-Rodriguez, Gordillo and Martinez-Bazan (2006) criticized their study by stating that the breakup time strongly depends on the initial position of the vortex core and that they failed to supply significant information about real dependence of the breakup time on the parameters of the problem.

Further recently, Revuelta (2010) performed full 3D simulations of the same and presented a better plot of particle breakup patterns for different size ratios (Figure 19), which the USF model had failed to account for.

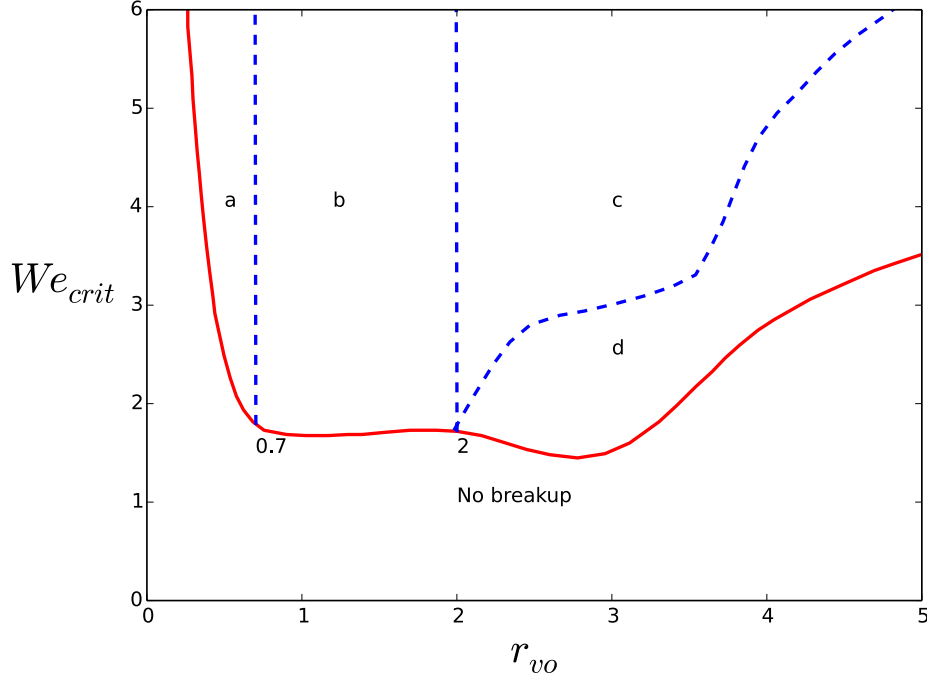


Figure 24: Critical Weber number We_{crit} vs the initial vortex-ring radius r_{vo} for $Re = 1000$, $\bar{\delta} = \frac{\delta}{a} = 0.05$. Region a: no binary breakup, no cigar formation, only satellite particles. Region b: lenticular deformation, multiple fragment breakup. Region c: lenticular formation, multiple similar size fragments, inverted U shape probability density function. Region d: cigar formation, U shape probability density function, binary non-similar size fragments. No breakup below the line [Redrawn from Figure 1 in Revuelta (2010)].

Critical Weber number obtained was in the same order as that of USF model. Hence this explains by far most of the phenomenon observed in experiments, though a non-aligned collision of a vortex ring and particle was not completely studied.

4.3. Resonance breakup

For the flows with $We > We_{crit}$, the parent particle breaks into two or more daughter particles and the relation derived for t_b (Equation 33) can be used to determine the approximate breakup time. But for sub-critical Weber numbers, individual turbulent eddies are not capable enough to break the interface, and the particle oscillates with an increasing frequency and decreasing amplitude as We decreases. However, the particle could still break due to previous deformation or fluctuating strength of the outer flow field. Hence the breakup depends on t_r (residence time), t_{rp} (particle response time), damping rate and turbulent time scales. This kind of breakup is referred to as resonance breakup.

Sevik and Park (1973) were the first to postulate resonance mechanism between the particle dynamics and the turbulent fluctuations. Later, Risso and Fabre (1998) coupled Rayleigh-Lamb theory (Lamb 1932 – valid up to breakup point) of particle oscillation with

the Kolmogorov-Hinze theory of turbulent breakup to explain interface deformation for a particle in a homogeneous turbulent field. Turbulent excitation was modeled with the same assumption as Kolmogorov-Hinze theory. Finally, they extended the Komogorov-Hinze theory for resonance breakup:

- a. (Weak turbulence) $WeC_d(t \rightarrow \infty) < \text{Critical value}$:
Individual eddies are not capable of causing breakup and accumulation of energy is not sufficient. So breakup is impossible.
- b. (Moderate turbulence) $WeC_d(t \rightarrow \infty) > \text{Critical value}$ and $WeC_d(t \rightarrow 0) < \text{Critical value}$:
Individual eddies are not capable of causing breakup, although a succession of turbulent eddies may be. Breakup is controlled by resonance like mechanism.
- c. (Intense turbulence) $WeC_d(t \rightarrow 0) > \text{Critical value}$:
Individual eddies are capable of causing sudden breakup of a previously non-deformed particle. Breakup agrees with force balance interpretation.

where C_d is mean efficiency coefficient, C_d depends on particle diameter and residence time of the particle.

Galinat et al. (2007) tested Risso and Fabre (1998)'s theory to the case of particle travelling through an inhomogeneous turbulent field and to that of concentrated particle dispersions and proved validity of the theory for a more general case. Revuelta, Rodriguez-Rodriguez and Martinez-Bazan (2006) numerically simulated the resonance breakup at sub-critical Weber number and observed that the particle deformation increases with the amplitude ζ of the external excitation. Residence time of particle (i.e. the time either particle breaks or manages to escape from the external flow) within the pure straining flow was found to decrease with the increase in ζ . The amplitude required for breakup ζ_b increases with the reduction of Re due to attenuation effect of the viscosity and ζ_b decreases as We increases towards critical value.

Further, Revuelta, Rodriguez-Rodriguez and Martinez-Bazan (2008) modelled turbulent breakup of particles at sub-critical Weber number using a 2D model of particle subjected to a pulsating USF with strain direction varying randomly for every pulse. They found that the relevant parameter that determines whether the particle breaks or not at a given time is the instantaneous surface energy which is directly correlated to the interfacial length, independently of the intensity of the outer flow or the detailed history of the deformation. When the frequency of the eddies train is similar to the oscillation frequency of the particle immersed in a steady USF whose Weber number is equal to the effective Weber number of the pulsating USF, they observed maximum breakup and breakup rate which is due to resonance. At sub-critical Weber number, they also observed similar characteristics in all breakup patterns: initially the particle adopts a cigar shape before taking the form of a dumb bell and finally breaks into fragments of approximately the same size. They also studied the effect of difference of angle between two consecutive strain directions: for an angle of around 90 deg, particle increases its level of deformation breaking up at values of critical surface energy whereas for angle of around 0 deg, no breakup is seen.

4.4. Breakup under the action of gravity:

Breakup of particles under the action of gravity in stagnant medium has already been covered in the Section 3.3 but for most of the present day practical (industrial) purposes, flow in a bubble column is generally governed both by the buoyancy and turbulence.

Until recently most of the studies concentrated on studying particle in a turbulent jet flow and pipe flows and accordingly modeling of these flows dealt with particle breakup assuming microgravity conditions. But Ravelet, Colin and Risso (2011), was the first to experimentally study the effect of buoyancy on the breakup of particles in turbulent flow. Assuming the gravity conditions for a flow in bubble column, buoyancy significantly affects the breakup mechanism due to relative slip between the particle and the external fluid.

According to the assumptions of the USF model, particle is moving at local mean fluid velocity (particle Reynolds number is zero) and the characteristic size of the particle lies within the inertial subrange of the turbulent energy spectrum. Hence the Reynolds number based on outer fluid properties of the flow surrounding the particle is sufficiently large to neglect the viscous effects. But this situation could be completely different for a particle rising in turbulent flow where the Reynolds number based on outer fluid properties is very low to neglect viscous effects and the particle Reynolds number is not zero but very high due to significant slip.

Characteristics of the flow and breakup in a turbulent bubble column are:

- Particle deformation dynamics is radically different from that observed in the absence of significant sliding motion due to buoyancy. Large deformations that lead to breakup are not axisymmetric.
- No trace of periodic oscillation at the eigen frequency f_2 , contrary to what is observed without buoyancy.
- Value of critical deformation leading to breakup is in agreement with results without buoyancy for particle in homogenous turbulence.
- The timescale of decay of shape oscillations is of order of their natural frequency f_2 , hence there is no stochastic resonance and breakup results only from the interaction with a single turbulent eddy.
- The magnitude of order of the instantaneous weber number was observed to be around 10.

Scaling of the particle breakup t_b was observed to be different depending on the interaction time t_i of the particle with a turbulent eddy:

- If t_i is short compared to $\frac{1}{f_2}$, t_b is proportional to $\frac{1}{f_2}$.
- If t_i is large compared to $\frac{1}{f_2}$, the forcing flow can be considered steady and USF model might be reasonable.

Further in turbulent flows, many other classification of flow types are observed, studied and reviewed. Experimental studies, theoretical breakup models and their derived correlations for drops and bubbles in turbulent pipe flows and in stirred vessels are few such examples. But these are considered beyond the scope of this article, since they are too problem specific and do not in general explain the actual physics of breakup process.

Nomenclature

a	Radius of the initially spherical particle / unperturbed jet (m)
Ar	Archimedes number
A^*	Relative difference of the projected area of the particle with respect to that of sphere (m^2)
A_{\max}^*	Maximum relative difference of the projected area of the particle with respect to that of sphere (m^2)
Bo	Bond number
B	Half-breadth of the particle (m)
Ca	Capillary number
C_d	Mean efficiency coefficient
d	Particle diameter (m)
d_d	Daughter particle diameter (m)
d_p	Parent particle diameter (m)
d_{\max}	Maximum stable particle diameter (m)
d_{o32}	Sauter mean diameter of the inviscid dispersed phase (m)
d_{32}	Sauter mean diameter of the dispersed phase (m)
D	Cross section diameter of the jet (m)
De	Deformation of the particle
D_H	Helix diameter (m)
D_i	Impeller diameter in stirred tanks (m)

D_t Pipe / tube diameter (m)
 Eo Eötvös number
 f_2 Eigen frequency of the second mode (s^{-1})
 g Acceleration due to gravity (ms^{-1})
 g^* Dimensionless breakup frequency
 G Shear rate (strength of shear flow) (s^{-1})
 Ga Galilei number
 g_c A conversion factor
 k Wavenumber (m^{-1})
 k_c Cut-off wavenumber (m^{-1})
 $l_{\frac{1}{2}}$ Initial half length of the particle (m)
 L Half-length of the particle (m)
 M Morton number
 n Growth rate of disturbance (\cdot)
 n_r Impeller speed (s^{-1})
 Oh Ohnesorge number
 P Pressure (Pa)
 r Radial coordinate (m)
 r_{vo} Initial vortex ring radius (m)
 Re Reynolds number
 R_v Vortex ring radius (m)
 R_{vp} Ratio of vortex ring radius to the particle radius

S_d A dimensional physical group t Time (s)
 t_b Breakup time or lifetime of the particle (s)
 t_i Interaction time of a particle with a turbulent eddy (s)
 t_r Particle residence time (s)
 t_t Characteristic turnover time of a turbulent eddy (s)
 t_r Particle response time (s)
 u mean velocity (ms^{-1})
 U Generic velocity scale (ms^{-1})
 u' fluctuation velocity (ms^{-1})
 U_M Terminal velocity of the drop at max diameter (ms^{-1})
 V Volume (m^3)
 We Weber number
 x Coordinate along main flow direction (m)
 y Coordinate normal to the wall (m)
 z Third spatial coordinate (m)
 α Flow type parameter
 Γ_∞ Upper bound to surfactant concentration ($molm^{-2}$)
 δ Vortex core radius (m)
 $\bar{\delta}$ Ratio of vortex core radius to the initial particle radius
 ε Turbulent dissipation (m^2s^{-3})
 ζ External excitation amplitude (m)

ζ_0 Initial perturbation amplitude (m)

ζ_b External excitation amplitude at breakup (m)

λ Viscosity ratio

μ Dynamic viscosity

ν Kinematic viscosity (m^2s^{-1})

ρ Density (kgm^{-3})

σ Surface tension (Nm^{-1})

τ Turbulent stress (Nm^{-2})

ω Growth rate of disturbance

Subscripts

crit critical value

c continuous phase

d dispersed phase

REFERENCES

- Acrivos, A & Lo, T, S 1978, 'Deformation and breakup of a slender drop in an extensional flow', J. Fluid Mech., Vol. 86, pp. 641-672.
- Acrivos, A 1983, 'The breakup of small drops and bubbles in shear flows', Ann. N. Y. Acad. Sci., Vol. 404, pp. 1-11.
- Arai, K, Konno, M, Matunga, Y & Saito, S, 1977, 'Effect of dispersed-phase viscosity on the maximum stable drop size for breakup in turbulent flow', J. Chem. Eng. Japan, Vol. 10, pp. 325-330.
- Ashgriz, N & Mashayek, F 1995, 'Temporal analysis of capillary jet breakup', J. Fluid Mech., Vol. 291, pp. 163-190.
- Ashgriz, N (ed.) 2011, 'Handbook of atomization and sprays', Springer.
- Barthes-Biesel, D 1972, PhD thesis, Stanford University.

- Barthes-Biesel, D & Acrivos, A 1973, 'Deformation and burst of a liquid droplet freely suspended in a linear shear field', *J. Fluid Mech.*, Vol. 61, part 1, pp. 1-21.
- Batchelor, G, K 1959, 'The theory of homogeneous turbulence', Cambridge University Press.
- Batchelor, G, K 1987, 'The stability of a large gas bubble rising through liquid', *J. Fluid Mech.*, Vol. 184, pp. 399-422.
- Bentley, B, J & Leal, L, G 1986, 'An experimental investigation of drop deformation and breakup in steady two-dimensional linear flows', *J. Fluid Mech.*, Vol. 61, pp. 1-21.
- Bhaga, D & Weber, M, E 1981, 'Bubbles in viscous liquids: shapes, wakes and velocities', *J. Fluid Mech.* Vol. 105, pp. 61-85.
- Bonometti, T & Magnaudet, J 2006, 'Transition from spherical cap to toroidal bubbles', *Phys. Fluids*, Vol. 18, pp. 1-12.
- Bousfield, D, W, Keunings, R, Marrucci, G & Denn, M, M 1986, 'Nonlinear analysis of the surface tension driven breakup of viscoelastic filaments', *J. Non-Newtonian Fluid Mech.*, Vol. 21, pp. 79-97.
- Bhaga, D & Weber, M, E 1981, 'Bubbles in viscous liquids: shapes, wakes and velocities', *J. Fluid Mech.*, Vol. 105, pp. 61-85.
- Buckmaster, J, D 1972, 'Pointer bubbles in slow viscous flow', *J. Fluid Mech.*, Vol. 55, pp.385-400.
- Buckmaster, J, D 1973, 'The bursting of pointer drops in slow viscous flow', *J. Appl. Mech.*, Vol. 40, pp. 18-24.
- Calabrese, R, V, Wang, C, Y & Bryner, N, P 1986, 'Drop breakup in turbulent stirred-tank contactors. Part 1: Effect of dispersed-phase viscosity', *AIChE J.*, Vol. 32, pp. 677-681.
- Cao, X, K, Sun, Z, G, Li, W, F, Liu, H, F, Yu, Z, H 2007, 'A new breakup regime for liquid drops identified in a continuous and uniform air jet flow', *Phys. Fluids*, Vol. 19(5), pp. 057103.
- Chhabra, R, P 2007, 'Bubbles, Drops, and Particles in Non-Newtonian Fluids', 2nded, Taylor & Francis.
- Chou, W,-H & Faeth, G, M 1998, 'Temporal properties of secondary drop breakup in the bag breakup regime', *Int. J. Multiphase Flow*, Vol. 24, pp. 889-912.
- Clift, R & Grace, J, R 1972, 'The mechanisms of bubble breakup in fluidized beds', *Ind. Eng. Chem. Fundam.*, Vol. 27, pp. 2309-2310.
- Clift, R, Grace, J, R & Weber, M, E 1974, 'Stability of bubbles in fluidized beds', *Ind. Eng. Chem. Fundam.*, Vol. 13, pp. 45-51.
- Clift, R, Grace, J, R, & Weber, M, E, 1978, 'Bubbles, drops and particles', Academic Press, Inc, New York.
- Cox, R, G 1969, 'The deformation of a drop in a general time-dependent fluid flow', *J. Fluid Mech.*, Vol. 37, pp. 601-623.
- Dai, Z, Faeth, G, M 2001, 'Temporal properties of secondary drop breakup in the multimode breakup regime', *Int. J. Multiphase Flow*, Vol. 27, pp. 217-236.
- Davies, J, T 1985, 'Drop sizes of emulsions related to turbulent energy dissipation rates', *Chem. Eng. Sci.*, Vol. 40, pp. 839-842.

- De Bruijn, R, A 1989, 'Deformation and breakup of drops in simple shear flows', PhD thesis, Tech. Univ. Eindhoven.
- De Bruijn, R, A 1993, 'Tipstreaming of drops in simple shear flows', Chem. Eng. Sci., Vol. 48, pp. 277-284.
- Delichatsios, M, A, 1975, 'Model for the breakup rate of spherical drops in an isotropic turbulent flows', Phys. Fluids, Vol. 18, pp. 622-623.
- Eggleton, C, D, Tsai, T & Stebe, K, J 2001, 'Tip streaming from a drop in the presence of surfactants', Phys. Rev. Lett., Vol. 87, Number 4, pp. 1-4.
- Feng J, Q 2010, 'A deformable liquid drop falling through quiescent gas at terminal velocity', J. Fluid Mech., Vol. 658, pp. 438-462.
- Frankel, N, A & Acrivos, A 1970, 'The constitutive equation for a dilute emulsion', J. Fluid Mech., Vol. 44, pp. 65-78.
- Galinat, S, Risso, F, Masbernat, O & Guiraud, P 2007, 'Dynamics of drop breakup in inhomogeneous turbulence at various volume fractions', J. Fluid Mech., Vol. 578, pp. 85-94.
- Gelfand, B, E 1996, 'Droplet Breakup Phenomena in Flows with Velocity Lag', Prog. Energy Comb. Sci., Vol. 22, pp. 201-265.
- Goren, S & Gavis, J 1961, 'Transverse wave motion on a thin capillary jet of a viscoelastic liquid', Phys. Fluids, Vol. 4, pp. 575-579.
- Grace, H, P 1971, 'Dispersion phenomena in high viscosity immiscible fluid systems and application of static mixers as dispersion devices in such systems', Eng. Found., Res. Conf. Mixing, 3rd, Andover, N. H., Republished in 1982, Chem. Eng. Com. Vol. 141, pp. 225-277.
- Grace, J, R, Wairegi, T & Brophy, J 1978, 'Break-up of drops in stagnant media', Can. J. Chem. Eng., Vol. 56, pp. 3-8.
- Guildenbecher, D, R 2009, 'Secondary Atomization of Electrostatically Charged Drops', PhD thesis, Purdue University.
- Guildenbecher, D, R, Lopez-Rivera & Sojka, P, E 2009, 'Secondary atomization', Exp Fluids, Vol. 46, pp. 371-402.
- Guildenbecher, D, R & Sojka, P, E 2011, 'Experimental investigation of aerodynamic fragmentation of liquid drops modified by electrostatic surface charge', Atom. Sprays, Vol. 21, pp. 139-147.
- Ha, J.-W & Yang, S.-M 2000, 'Deformation and breakup of Newtonian and non-Newtonian conducting drops in an electric field', J. Fluid Mech., Vol. 405, pp. 131-156.
- Haas, F, C, 1964, 'Stability of droplets suddenly exposed to a high velocity gas stream', AIChE J., Vol. 10, pp. 920-924.
- Han, J, Tryggvason, G 1999, 'Secondary breakup of axisymmetric liquid drops. I. Acceleration by a constant body force', Physics of Fluids, Vol. 11(12), pp. 3650-3667.
- Han, J, Tryggvason, G 2001, 'Secondary breakup of axisymmetric liquid drops. II. Impulsive acceleration', Phys. Fluids, Vol. 13(6), pp. 1554-1565.
- Hanson, A, R, Domich, E, G & Adams, H, S 1963, 'Shock-tube investigation of the breakup of drops by air blasts', Phys. Fluids, Vol. 6, pp. 1070-1080.
- Hesketh, R, P, Russell, T, W, F & Etchells, A, W 1987, 'Bubble size in horizontal pipelines', AIChE J., Vol. 33, pp. 663-667.

- Hesketh, R, P, Etchells, A, W & Russell, T, W, F 1991a, 'Bubble breakage in pipeline flow', *Chem. Eng. Res.*, Vol. 46, pp. 1-9.
- Hesketh, R, P, Etchells, A, W & Russell, T, W, F 1991b, 'Experimental observations of bubble breakage in turbulent flow', *Ind. Eng. Chem. Res.*, Vol. 30, pp. 835-841.
- Higuera, F, J 2004, 'Axisymmetric inviscid interaction of a bubble and a vortex ring', *Phys. Fluids*, Vol. 16, No. 4, pp. 1156-1159.
- Hinch, E, J & Acrivos, A 1979, 'Steady long slender droplets in two-dimensional straining motion', *J. Fluid Mech.*, Vol. 91, pp. 401-414.
- Hinch, E, J & Acrivos, A 1980, 'Long slender drops in a simple shear flow', *J. Fluid Mech.*, Vol. 98, pp. 308-328.
- Hinze, J, O 1955, 'Fundamentals of the hydrodynamic mechanism of splitting in dispersion processes', *AIChE J.*, Vol. 1, pp. 289-295.
- Hsiang, L, P & Faeth, G, M 1992, 'Near-limit deformation and secondary breakup', *Int. J. Multiphase Flow*, Vol. 18, pp. 635-652.
- Hu, S & Kinter, R, G 1955, 'The fall of single liquid drops through water', *AIChE J.*, Vol. 1, pp. 43-49.
- Jain, M, Prakash, R, S, Tomar, G & Ravikrishna, R, V 2015, 'Secondary breakup of a drop moderate Weber numbers', *Proc. R. Soc. A*, Vol. 471, pp. 1-25.
- Jain, S, S, Tyagi, N, Tomar, G, Prakash, R, S, Ravikrishna, R, V & Raghunandhan, B, N 2016 'Effect of Density Ratio on the Secondary Breakup of Spherical Drops in a Gas Flow', Presented at 18th Annual Conference of Liquid Atomization & Spray Systems - Asia, Chennai, India (ILASS - Asia 2016)
- Jain, S, S, Tyagi, N, Tomar, G, Prakash, R, S, Ravikrishna, R, V & Raghunandhan, B, N 2017 'Density ratio and Reynolds number effect in the Secondary breakup of drops at moderate Weber numbers', Manuscript under preparation.
- Janssen, J, J, M, Boon, A & Agterof, W, G, M 1994, 'Influence of dynamic interfacial properties on droplet breakup in simple-shear flow', *AIChE J.*, Vol. 40, pp. 1929-1939.
- Janssen, J, J, M, Boon, A & Agterof, W, G, M 1997, 'Influence of dynamic interfacial properties on droplet breakup in plane hyperbolic flow', *AIChE J.*, Vol. 43, pp. 1436-1447.
- Kang, I, S & Leal, L, G 1987, 'Numerical solution of axisymmetric, unsteady free-boundary problems at finite Reynolds number. I. Finite difference scheme and its application to the deformation of a bubble in a uniaxial straining flow', *Phys. Fluids*, Vol. 30, pp. 1929-1940.
- Kang, I, S & Leal, L, G 1989, 'Numerical solution of axisymmetric, unsteady free-boundary problems at finite Reynolds number. II. Deformation of a bubble in a biaxial straining flow', *Phys. Fluids A*, Vol. 1, pp. 644-660.
- Kang, I, S & Leal, L, G 1990, 'Bubble dynamics in time-periodic straining flows', *J. Fluid Mech.*, Vol. 218, pp. 41-69.
- Kkesi, T, Amberg, G & Wittberg, L, P 2014, 'Drop deformation and breakup', *Int. J. Multiphase Flow*, Vol. 66, pp. 1-10.
- Kkesi, T, Amberg, G & Wittberg, L, P 2016, 'Drop deformation and breakup in flows with shear', *Chem. Eng. Sci.*, Vol. 140, pp. 319-329.

- Khakar, D, V & Ottino, J, M 1987, 'Breakup of liquid threads in linear flows', *Int. J. Multiphase Flow*, Vol. 13, pp. 147-180.
- Klett, J, D 1971, 'On the breakup of water drops in air', *J. Atmos. Sci.*, Vol. 28, pp. 646-647.
- Kolmogorov, A, N, 1949, 'On the disintegration of drops in a turbulent flow', *Doklady Akad. Nauk.*, Vol. 66, pp. 825-828.
- Komabayasi, M, Gonda, T & Isono, K 1964, 'Life time of water drops before breaking and size distribution of fragments droplets', *J. Met. Soc. Japan*, Vol. 42, pp. 330-340.
- Komrakova, A, Shardt, O, Eskin, D, Derksen, J 2015, 'Effects of dispersed phase viscosity on drop deformation and breakup in inertial shear flow', *Chem. Eng. Sci.*, Vol. 126, pp. 150-159.
- Krishna, P, M, Venkateswarlu, D & Narasimhamurty, G, S, R 1959, 'Fall of liquid drop in water, drag coefficients, peak velocities and maximum drop sizes', *J. Chem. Engng Data*, Vol. 4, pp. 340-343.
- Kubie, J. & Gardner, G, C 1977, 'Drop sizes and drop dispersion in straight horizontal tubes and in helical coils', *Chem. Eng. Sci.*, Vol. 32, pp. 195-202.
- Lamb, H, 1932, 'Hydrodynamics', Cambridge University Press.
- Lane, W, R 1951, 'Shatter of drops in streams of air', *Ind. Eng. Chem.*, Vol. 43, pp. 1312-1317.
- Levich, V, G 1962, 'Physico-chemical hydrodynamics', Prentice-Hall, Englewood Cliffs. N. J.
- Lewis, D, A & Davidson, J, F 1982, 'Bubble splitting in shear flow', *Trans. IChemE*, Vol. 60, pp. 283-291.
- Li, J, Renardy, Y, Renardy, M, 2000, 'Numerical simulation of breakup of a viscous drop in simple shear flow through a volume-of-fluid method', *Phys. Fluids*, Vol. 12 (2), pp. 269-282.
- Liao, Y & Lucas, D, 2009, 'A literature review of theoretical models for drop and bubble breakup in turbulent dispersions', *Chem. Eng. Sci.*, Vol. 64, pp. 3389-3406.
- Liao, Y & Lucas, D, 2010, 'A literature review on mechanisms and models for the coalescence process of fluid particles', *Chem. Eng. Sci.*, Vol. 65, pp. 2851-2864.
- Liao, Y, Lucas, D, Krepper, E & Schmidke, M 2011, 'Development of a generalized coalescence and breakup closure for the inhomogeneous MUSIG model', *Nuclear Engineering and Design*, Vol. 241, pp. 1024-1033.
- Liu, Z, Reitz, R, D 1997, 'An analysis of the distortion and breakup mechanisms of high speed liquid drops', *Int. J. Multiphase Flow*, Vol. 23(4), pp. 631-650.
- Martinez-Bazan, C, Montanes, J, J & Lasheras, J, C 1999, 'On the breakup of an air bubble injected into a fully developed turbulent flow. Part 1. Breakup frequency', *J. Fluid Mech.*, Vol. 401, pp. 157-182.
- Mikami, T, Cox, R & Mason, S, G 1975, 'Breakup of extending liquid threads', *Int. J. Multiphase Flow*, Vol. 2, pp. 113-138.
- Miskis, M, A 1981, 'A bubble in an axially symmetric shear flow', *Phys. Fluids*, Vol. 24, pp. 1229-1231.

Ohta, M, Imura, T, Yoshida, Y & Sussman, M 2005, 'A computational study of the effect of initial bubble conditions on the motion of a gas bubble rising in viscous liquids', *Int. J. Multiphase Flow*, Vol. 31, pp. 223-237.

Padrino, J, C & Joseph, D, D 2011, 'Viscous irrotational analysis of the deformation and break-up time of a bubble or drop in uniaxial straining flow', *J. Fluid Mech.*, Vol. 688, pp. 390-421.

Paul, H, I & Sleicher, C, A 1965, 'The maximum stable drop size in turbulent flow: effect of pipe diameter', *Chem. Eng. Sci.*, Vol. 20, pp. 57-59.

Pilsh, M & Erdman, C, A 1987, 'Use of breakup time data velocity history data to predict the maximum size of stable fragments for acceleration-induced breakup of a liquid drop', *Int. J. Multiphase Flow*, Vol. 13, pp. 741-757.

Pimbley, W, T & Lee, H, C 1977, 'Satellite droplet formation in a liquid jet', *IBM J. Res. Dev.*, Vol. 21, pp. 21-30.

Plateau, J 1873, 'Statique experimentale et theorique des liquids soumis aux seules forces moleculaires', Cited by Rayleigh, L 1945, 'Theory of Sound', Vol. 2, pp. 363. New York: Dover.

Ponstein, J 1959, 'Instability of rotating cylindrical jets', *Appl. Sci. Res.*, Vol. 8, pp. 425-456.

Prakash, R, S, Jain, S, S, Tomar, G, Ravikrishna, R, V, Raghunandhan, B, N 2016 'Computational study of liquid jet breakup in swirling cross flow', Presented at 18th Annual Conference of Liquid Atomization & Spray Systems - Asia, Chennai, India (ILASS - Asia 2016)

Qian, D, McLaughlin, J, B, Sankaranarayanan, K, Sundaresan, S & Kontomaris, K 2006, 'Simulation of bubble breakup dynamics in homogeneous turbulence', *Chem. Eng. Comm.*, Vol. 193, pp. 1038-1063.

Rallison, J, M & Acrivos, A 1978, 'A numerical study of the deformation and burst of a viscous drop in an extensional flow', *J. Fluid Mech.*, Vol. 89, pp. 191-200.

Rallison, J, M 1981, 'A numerical study of the deformation and burst of a viscous drop in general shear flows', *J. Fluid Mech.*, Vol. 109, pp. 465-482.

Rallison, J, M 1984, 'The deformation of small viscous drops and bubbles in shear flows', *Ann. Rev. Fluid Mech.*, Vol. 16, pp. 45-66.

Ravelet, F, Colin, C and Risso, F 2011, 'On the dynamics and breakup of a bubble rising in a turbulent flow', *Physics of Fluids*, Vol. 23, pp. 1-12.

Rayleigh, L 1878, 'On the instability of jets', *Proc. London Math. Soc.*, pp. 4-13.

Rayleigh, L 1892, 'On the instability of cylindrical fluid surfaces', *Phil. Mag*, Vol. 34, pp. 177-180.

Renardy, Y, Cristini, V, 2001a, 'Effect of inertia on drop breakup under shear', *Phys. Fluids*, Vol. 13(1), pp. 7-13.

Renardy, Y, Cristini, V, 2001b, 'Scalings for fragments produced from drop breakup in shear flow with inertia', *Phys. Fluids*, Vol. 13(8), pp. 2161-2164.

Renardy, Y, Cristini, V, Li, J, 2002, 'Drop fragment distributions under shear with inertia', *Int. J. Multiphase Flow*, Vol. 28, pp. 1125-1147.

- Renardy, Y, 2008, 'Effect of startup conditions on drop breakup under shear with inertia', *Int. J. Multiphase Flow*, Vol. 34, pp. 1185–1189.
- Revuelta, A, Rodriguez-Rodriguez, J & Martinez-Bazan, C 2006, 'Bubble break-up in a straining flow at finite Reynolds numbers', *J. Fluid Mech.*, Vol. 551, pp. 175-184.
- Revuelta, A, Rodriguez-Rodriguez, J & Martinez-Bazan, C 2008, 'On the breakup of bubbles at high Reynolds numbers and subcritical Weber number', *Eur. J. Mech. B/Fluids*, Vol. 27, pp. 591-608.
- Revuelta, A 2010, 'On the interaction of a bubble and a vortex ring at high Reynolds numbers', *Eur. J. Mech. B/Fluids*, Vol. 29, pp. 119-126.
- Rimbert, N & Castanet, G 2011, 'Crossover between Rayleigh-Taylor instability and turbulent cascading atomization mechanism in the bag-breakup regime', *Phys. Rev. E*, Vol. 84.
- Risso, F & Fabre, J 1998, 'Oscillations and breakup of a bubble immersed in a turbulent field', *J. Fluid Mech.*, Vol. 372, pp. 323-355.
- Risso, F 2000, 'The mechanisms of deformation and breakup of drops and bubbles', *Multiphase Sci. Technol.*, Vol. 12, pp. 1-50.
- Rodriguez-Rodriguez, J, Gordillo, J, M & Martinez-Bazan, C 2006, 'Breakup time and morphology of drops and bubbles in a high-Reynolds-number flow', *J. Fluid Mech.*, Vol. 548, pp. 69-86.
- Rumscheidt, F, D & Mason, S, G 1961, 'Particle motions in sheared suspensions. XII. Deformation and burst of fluid drops in shear and hyperbolic flows', *J. Colloid Interf. Sci.*, Vol. 16, pp. 238-261.
- Rumscheidt, F, D & Mason, S, G 1962, 'Break-up of stationary liquid threads', *J. Colloid Science*, Vol. 17, pp. 260-269.
- Rutland, D, F & Jameson, G, J 1970, 'Theoretical prediction of the sizes of drops formed in the breakup of capillary jets', *Chem. Eng. Sci.*, Vol. 25, pp. 1689–1698.
- Ryan, R, T 1978, 'The possible modification of convective systems by the use of surfactants', *J. Appl. Met.*, Vol. 15, pp. 3-8.
- Ryskin, G & Leal, L, G 1984, 'Numerical solution of free-boundary problems in fluid mechanics. Part 3. Bubble deformation in an axisymmetric straining flow', *J. Fluid Mech.*, Vol. 148, pp. 37-43.
- Sathyagal, A, N, Ramkrishna, D & Narsimhan, G 1996, 'Droplet breakage in stirred dispersions. Breakage functions from experimental drop-size distributions', *Chem. Eng. Sci.*, Vol. 51, pp. 1377-1391.
- Sevik, M & Park, S, H 1973, 'The splitting of drops and bubbles by turbulent fluid flow', *J. Fluids Engng.*, pp. 53-60.
- Shinnar, R 1961, 'On the behavior of liquid dispersions in mixing vessels', *J. Fluid Mech.*, Vol. 10, pp. 259-275.
- Sleicher, C, A 1962, 'Maximum stable drop size in turbulent flow', *AIChE J.*, Vol. 8, pp. 471-477.
- Solsvik, J, Tangen, S & Jakobsen, H A 2013 'On the constitutive equations for fluid particle breakage', *Rev. Chem. Eng.*, Vol. 29, pp. 241-356.

- Spangler, C, A, Hibling, J, H & Heister, S, D, 'Nonlinear modeling of jet atomization in the wind-induced regime', *Phys. Fluids*, Vol. 7(5), pp. 964-971.
- Stone, H, A, Bentley, B, J & Leal, L, G 1986, 'An experimental study of transient effects in the breakup of viscous drops', *J. Fluid Mech.*, Vol. 173, pp. 131-158.
- Stone, H, A & Leal, L, G 1989, 'Relaxation and breakup of an initially extended drop in an otherwise quiescent fluid', *J. Fluid Mech.*, Vol. 198, pp. 399-427.
- Stone, H. A. & Leal, L. G 1990, 'The effects of surfactants on drop deformation and breakup', *J. Fluid Mech.*, Vol. 220, pp. 161-186.
- Stone, H, A 1994, 'Dynamics of drop deformation and breakup in viscous fluids', *Annu. Rev. Fluid Mech.*, Vol. 26, pp. 65-102.
- Taylor, G, I 1932, 'The viscosity of a fluid containing small drops of another fluid', *Proc. R. Soc. A*, Vol. 138, pp. 41-48.
- Taylor, G, I 1934, 'The formation of emulsions in definable fields of flow', *Proc. R. Soc. A*, Vol. 146, pp. 501-523.
- Taylor, G, I 1964, 'Conical free surfaces and fluid interfaces', *Proc. Int. Cong. Of Appl. Mech.*, 11th, Munich, pp. 790-796.
- Tjahjadi, M, Stone, H, A & Ottino, J, M 1992, 'Satellite and subsatellite formation in capillary breakup', *J. Fluid Mech.*, Vol. 243, pp. 297-317.
- Tomotika, S 1935, 'On the stability of a cylindrical thread of a viscous liquid surrounded by another viscous fluid', *Proc. R. Soc. Lond. Ser. A*, Vol. 150, pp. 322-337.
- Tomotika, S 1936, 'Breaking up of a drop of viscous liquid immersed in another viscous fluid which is extending at a uniform rate', *Proc. R. Soc. Lond. Ser. A*, Vol. 153, pp. 302-318.
- Torza, S, Cox, R, G & Mason, S, G 1972, 'Particle motions in sheared suspension. XXVII. Transient and steady deformation and burst of liquid drops', *J. Colloid Int. Sci.*, Vol. 38, pp. 395-411.
- Tripathi, M, K, Sahu, K, C & Govindarajan, R 2015, 'Dynamics of an initially spherical bubble rising in quiescent liquid', *Nature Communications*, Vol. 6, pp. 1-9.
- Wallis, G, B 1969, 'One-dimensional two-phase flow', McGraw Hill.
- Walter, J, F & Blanch, H, W 1986, 'Bubble break-up in gas-liquid bioreactors: break-up in turbulent flows', *Chem. Eng. J.*, Vol. 32, pp. 7-17.
- Weber, C 1931, 'On the breakdown of a fluid jet, Zum Zerfall eines Flüssigkeitsstrahles', *Z. Angew. Math. und Mech.*, Vol. 11, pp. 136-154.
- Xiao, F, Dianat, M, & McGuirk, J, J 2014, 'Large eddy simulation of single droplet and liquid jet primary breakup using a coupled level set/ volume of fluid method', *Atomization Spray*, Vol. 24, pp. 281-302.
- Youngren, G, K & Acrivos, A 1976, 'On the shape of a gas bubble in a viscous extensional flow', *J. Fluid Mech.*, Vol. 76, pp. 433-442.
- Yu, K , L 1974, PhD thesis, University of Houston.